

C-Glycoside Mimetics Inhibit Glioma Stem Cell Proliferation, Migration, and Invasion

Ludovic Clarion,^{†,⊥} Carine Jacquard,^{‡,⊥} Odile Sainte-Catherine,[§] Marc Decoux,[†] Séverine Loiseau,[†] Marc Rolland,^{||} Marc Lecouvey,[§] Jean-Philippe Hugnot,[‡] Jean-Noël Volle,[†] David Virieux,[†] Jean-Luc Pirat,^{*,†} and Norbert Bakalara^{*,‡}

[†]UMR 5253—ICG Montpellier, Equipe AM₂N, ENSCM, 8, Rue de l'École Normale, 34296 Montpellier CEDEX 5, France

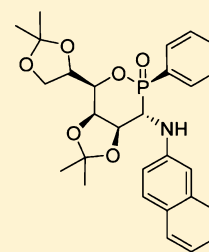
[‡]INSERM U-1051, Institut des Neurosciences de Montpellier, 80 Rue Augustin Fliche, 34091 Montpellier, France

[§]UMR 7244 CSPBAT, Equipe CBS Université Paris 13, 74 Rue Marcel Cachin, 93017 Bobigny CEDEX, France

^{||}Institut Européen des Membranes, cc047 Université de Montpellier 2, 34095, Montpellier, France

Supporting Information

ABSTRACT: This paper reports the design and synthesis of C-glycoside mimetics (D-glycero-D-talo- and D-glycero-D-galactopyranose analogues), a subset of the recently published phostines, belonging to the [1,2]oxaphosphinane core. Eighteen new compounds were tested against 11 cancer cell types belonging to six categories of tumor tissues and three different species. The hit compound **5.3d** inhibited invasion and migration of both GBM stem cells (Gli7 and Gli4) and GBM cancer cell lines (C6, SNB75) on fibronectin, vitronectin, and laminin. K_i values for Gli7 and Gli4 migration inhibition on fibronectin were 16 and 31 nM respectively. K_i values for invasion inhibition in a 3D system were 46 nM for Gli7 and 290 nM for Gli4. These activities were associated with an antiproliferative effect on Gli4 ($EC_{50} = 5.20 \mu\text{M}$) and Gli7 ($EC_{50} = 2.33 \mu\text{M}$). In conclusion, the heptopyranose mimetic **5.3d**, devoid of toxicity on astrocyte and cortical neuron cultures at concentrations below 100 μM , opens new therapeutic perspectives against glioblastoma.



1. INTRODUCTION

Gliomas are the most common primary central nervous system (CNS) tumors. They account for over 40% of CNS tumors and 78% of CNS malignancies in adults.¹ The median survival is only 12–15 months for patients with glioblastomas (GBMs, WHO grade IV), 2–5 years for patients with anaplastic gliomas (WHO grade III), and 4–10 years for patients with low-grade gliomas (LGG, including WHO grades I and II). Surgery with maximal resection is the first therapeutic option in both low-grade and high-grade gliomas.^{1,2} To this end, because of the diffuse nature of gliomas, it has recently been proposed to perform, when possible, a supratotal resection, that is, to remove a margin around the tumor visible on FLAIR-weighted MRI.³ However, optimal glioma removal is not always possible because of the invasion of eloquent structures⁴ and the dispersion of migrating glioma cells in the brain even over long distances.⁵ The resulting recurrent lesions are responsible for the fatal outcome of the disease, and it has been recently published in a murine model that migration precedes tumor mass formation of glioma cells overexpressing H-RAS.⁶ Interestingly, a microarray analysis of laser capture-microdissected glioma cells reveals respectively two transcriptional profiles corresponding to cells collected from patient tumor cores and white matter-invading cells. The profile corresponding to invading cells is thought to represent in part a gene migration signature.^{7,8} From an oncologic point of view, most studies on glioma therapies in the past decades investigated proliferation, whereas migration has received less attention. Therefore, invasive GBM cells are unlikely to respond to conventional therapies based on studies of proliferative and

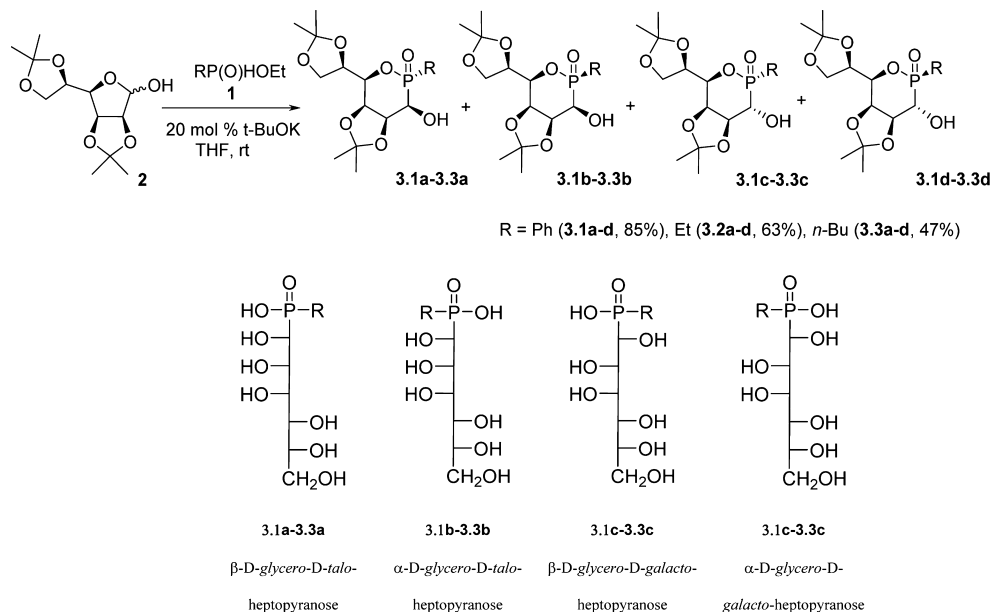
stationary cells of the tumoral mass that has been the reference tissue for the molecular genetics of this disease.⁷ Therefore, it has recently been suggested to develop innovative neoadjuvant antimigratory chemotherapies to limit expansion of the tumor and to allow a greater efficiency of surgery.⁸

Receptors, signaling pathways, and transcription factors regulating migration have already been characterized in GBM.^{9,10} PI3K and MAPK pathway deregulation has been linked with increased cellular motility via EGFR signaling in GBM.¹¹ Amplification and/or overexpression of the HGF/MET pathway has also been implicated in GBM invasion, leading to clinical trials of MET inhibitors.¹² However, therapeutic strategies based on inhibition of signaling pathways suffer from the redundant regulation of signaling nodes, which allows shifting responses to inhibition of a specific pathway. Moreover, because these signaling pathways are also active in nontumoral cells, severe toxicity is often observed.

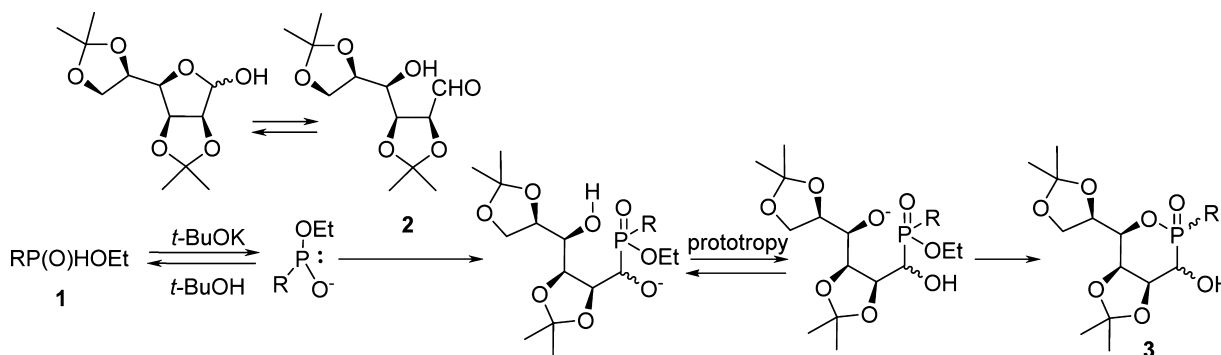
In this context, we took the initiative to design and synthesize a family of compounds screened not only for their antiproliferative activity but also for their antimigration and invasion inhibition properties. This new family of glycomimetics, analogues of hexopyranoses,¹³ was named the phostines. We hypothesized that such a new class of compounds would impact cellular pathways different from the commonly studied targets of antitumor drugs.^{7–10} In the past decades, numerous phosphonosugars, in which the anomeric carbon of a furanose or pyranose

Received: April 2, 2014

Scheme 1. Synthetic Route to Hydroxyoxaphosphinanes 3



Scheme 2. Mechanism of Formation of the 3-Hydroxyoxaphosphinanes 3



ring is replaced by a phosphonic group, have been advanced as potent therapeutic agents.¹⁴ We previously published a hit compound displaying stereospecific antiproliferative properties against CNS cell lines and devoid of toxicity on normal astrocytes.¹³ A comparison analysis performed using NCI/NIH software indicated that it interfered with a biochemical process that has not yet been targeted by any standard anticancer agent.¹³ In our quest to identify new anticancer families, we have extended the phostine family by the synthesis of 19 new phosphinosugars in which the anomeric carbon of a *D*-glycero-*D*-talo-heptopyranose or *D*-glycero-*D*-galacto-heptopyranose ring was replaced by a phosphinate function. In the present work, the antiproliferative properties of these new phostines against nine different cancer cell lines and two GBM stem cell cultures were determined. Subsequently, the antimigratory effects of two selected compounds, 3.2a and 5.3d, were evaluated against the GBM cell lines and two GBM stem cell cultures. The toxicity of the selected compound 5.3d was assessed against mouse primary cultures of neurons and astrocytes. This study showed that 5.3d is an antiproliferative compound affecting cultured primary GBM cell migration and is devoid of toxicity when used below 100 μ M on neuronal and glial cells.

2. RESULTS

2.1. Phostines Synthesis. These new *D*-glycero-*D*-talo-heptopyranose or *D*-glycero-*D*-galacto-heptopyranose analogues can be seen as a combination of glycopyranosides and *C*-arylglycosides. Their synthesis was achieved by the reaction of 2,3,5,6-di-*O*-isopropylidene- α -*D*-mannofuranose 2 with various ethyl alkylphosphinates (Et or *n*-Bu) or methyl phenylphosphinate 1 in the presence of a catalytic amount of potassium *tert*-butoxide (Scheme 1).

This first sequence involved the nucleophilic Pudovik addition of *H*-phosphinate anions to the open-chain form of mannofuranose 2. The second step consisted of a subsequent prototropy followed by a 6-exotet cyclization, affording the six-membered ring phosphinolactones (Scheme 2).

This procedure offered an easy tuning of the alkyl or aryl substituent directly bound to the phosphorus atom. In the case of R = Ph, three diastereomers 3.1a–3.1c (Table 1) were isolated; diastereomer 3.1a ($\delta = 30.42$ ppm) was readily recovered because of its precipitation into the reaction mixture (yield about 30%). Furthermore, two other diastereomers, 3.1b ($\delta = 40.03$ ppm) and 3.1d ($\delta = 36.21$ ppm), were successfully isolated after successive purification on column chromatography and recrystallization, with respectively 17% and 4% yields. When R group is an alkyl (Et or Bu), a mixture of three diastereomers for

Table 1. Structures of Phostines

Structure					
Compounds	3.1a	3.1b	3.1d		
Structure					
Compounds	3.2a	3.3a	4.1a	4.2a	4.3a
Structure					
Compounds	4.4a	4.5a	4.6a	4.7a	5.1d
Structure					
Compounds	5.2d	5.3d	5.4d	5.5d	5.6d

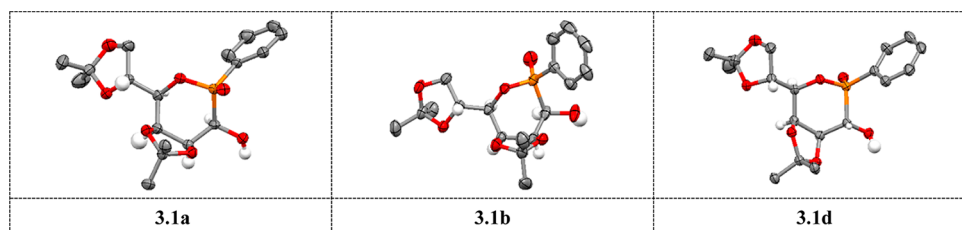
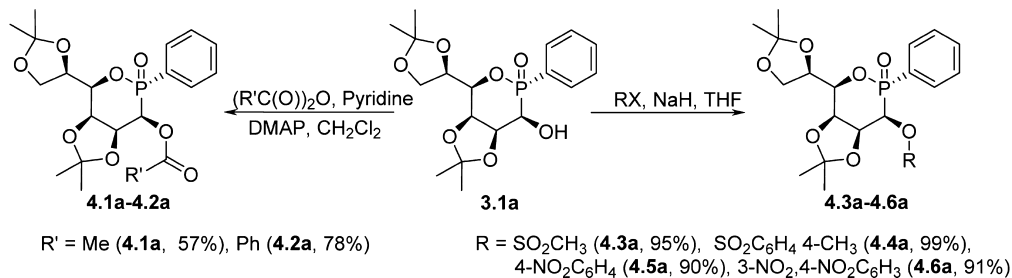
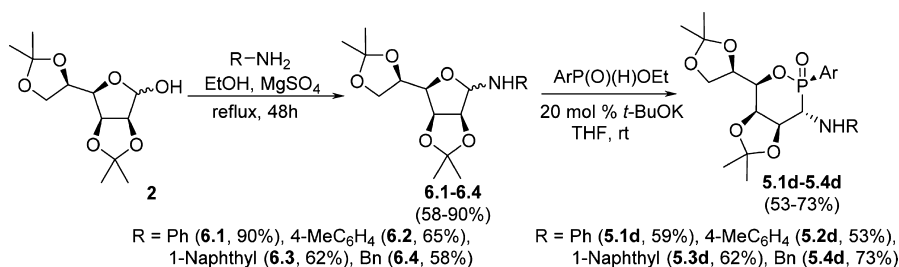


Figure 1. ORTEP structures of compounds 3.1a, 3.1b, and 3.1d based on diffraction analyses.

Scheme 3. Synthesis of the β -D-glycero-D-talo-Pyranose Analogues 4.1a–4.2a and 4.3a–4.6a

3.2 (Et) and 3.3 (Bu) was observed in an overall yield approximately 63% and 47% calculated by ^{31}P NMR.

Suitable crystals for X-ray analysis were obtained for the three diastereomers. According to the ORTEP structure, the absolute

Scheme 4. Synthetic Routes of the *D*-glycero-*D*-talo- or *D*-glycero-*D*-Galactopyranose Analogues 5.1d–5.4d

configuration of the newly created asymmetric centers for diastereomers **3.1a**, **3.1b**, and **3.1d** was assigned (Figure 1).¹⁵ The crystals for phosphinosugar **3.1a** were obtained from chloroform/acetone (1/2) and showed a correspondence with the *D*-glycero- β -*D*-talo-heptopyranose. The structure adopted a slightly twisted boat conformation with $P_2(S)$, $C_3(R)$ configurations. Crystals of phostine **3.1b** were obtained in diethyl ether/heptane (2/1), allowing the attribution of the *D*-glycero- α -*D*-talo-heptopyranose structure with a boatlike conformation and the $P_2(R)$, $C_3(R)$ configurations. The third phosphine, **3.1d**, was attributed to the *D*-glycero- α -*D*-galacto-heptopyranose analogue by crystallization in diethyl ether/pentane (2/1) and exhibited a chair conformation with $P_2(R)$, $C_3(S)$ configuration. We also modified the hydroxyl group in order to determine whether or not hydrogen bonding in this position affects the activity. For this purpose, the corresponding ester and ether derivatives were synthesized starting from the *D*-glycero- β -*D*-talo-heptopyranose **3.1a** by acylation or Williamson reactions (Scheme 3). The mesylate **4.3a** and tosylate **4.4a** were obtained respectively in 95% and quantitative yield by reaction with the corresponding sulfonyl chloride, but no further nucleophilic substitution was effective because of high steric hindrance at this position. The amino derivative **4.7a** (R = 4-H₂NC₆H₄) was synthesized, with a yield of 96%, by reduction of the nitro group, starting from the stereoisomer **4.5a** using hydrogen and Pd/C catalyst.

Direct synthesis of 3-amino-1,2-oxaphosphinanes **5.1–5.4** can be performed starting from alkylaminomannofuranoses or arylaminomannofuranoses. Thus, **6.1** (R = Ph), **6.2** (R = 4-MeC₆H₄), **6.3** (R = 1-naphthyl), and **6.4** (R = Bn) were quantitatively produced by treatment of 2,3,5,6-di-*O*-isopropylidene- α -*D*-mannofuranose **2** with respectively an excess of aniline, *p*-toluidine, 1-naphthylamine, or benzylamine.^{16,17} Then the phostines **5.1–5.4** were synthesized using the reaction conditions mentioned above. For the benzylamino derivative, only one stereoisomer **5.4d**, among the four possible ones, was isolated (73% yield) after purification by chromatography (Scheme 4).

Suitable crystals for X-ray analysis were obtained from hexane for compound **5.4d**. According to the ORTEP structure, the absolute configuration of the new created asymmetric centers of the diastereomer **5.4d** was successfully assigned (Figure 2). The phosphinosugar **5.4d**, a *D*-glycero- α -*D*-galacto-heptopyranose analogue, showed a boat structure with $P_2(R)$, $C_3(S)$ configurations. Hydrogenolysis of the *N*-benzyl phosphinate **5.4d** was achieved using hydrogen and Pd/C catalyst and led to the amino derivative **5.5d** at a yield of 87% (Scheme 4).

The nonoptimized transformation of the aminophostine **5.5d** into the amidophostine **5.6d** was achieved using acetic anhydride and triethylamine in 12% yield (Scheme 5).

2.2. Among the New P-Glycoside Family, 10 Compounds Exhibit an Antiproliferative Activity against the

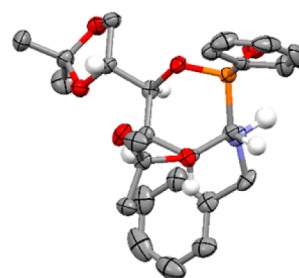


Figure 2. ORTEP structure of compound **5.4d** based on diffraction analyses.

Cell Lines and Primary Cultures of Rat and Human GBM.

Phostines were screened on a panel of 11 cancer cell types from three species derived from six different types of cancer tissue. The panel comprised (Table 2) human GBM cancer stem cells (Gli4, Gli7), human (SNB75) and rat (C6) GBM cell lines; human (MDAMB435) and mouse (B16F10) melanoma cell lines; human epidermoid cell line (A431); human hepatocarcinoma cell line (HuH7); human colorectal carcinoma cell line (CaCo2); prostatic carcinoma cell line (DU-145); and human breast adenocarcinoma (pleural metastasis) cell line (MDAMB231). To evaluate the antiproliferative activity of 18 *D*-glycero-*D*-talo- and *D*-glycero-*D*-galactopyranoses, we have used a MTT test and fixed an EC₅₀ cut-off value of 10 μ M for compounds selection. Ten compounds, **3.2a**, **3.3a**, **4.2a**, **4.3a**, **4.4a**, **4.6a**, **4.7a**, **5.2d**, **5.3d**, and **5.6d** (Table 2), were identified as potent hits with IC₅₀ lower than 10 μ M on GBM cancer stem cells (Gli4 and Gli7) and GBM cell lines (SNB75 and C6). Interestingly, within this subset of 10 compounds, only one (**3.2a**) exhibited an antiproliferative activity restricted to glioblastoma (Table 2). This brain cancer tissue specificity of **3.2a** was reinforced by the absence of toxicity against DU145 (IC₅₀ > 100 μ M) differentiating the behavior of such compound between GBM and metastatic brain tumors. The nine others compounds did not show any tissue specific antiproliferative activity (Table 2). Among these compounds, **5.3d** was the only one to be active against cancer cell lines derived at least from three other tissues: skin cancer cell lines (MDAMB435, A431), breast cancer cell line (MDAMB231), and liver cancer cell line (HuH7). Interestingly, CaCo2, commonly used to evaluate metabolism of compounds by the intestine, was insensitive to the 18 compounds.

Therefore, in a second screening step, in order to select a hit compound inhibiting glioma cell migration and invasion, we made the choice to evaluate *D*-glycero-*D*-talo-heptopyranose **3.2a** and *D*-glycero-*D*-galacto-heptopyranose **5.3d** because of the opposition existing between the brain tissue specificity of **3.2a** and the extended antiproliferative activities of **5.3d**.

2.3. Antimigratory Activity of 5.3d and 3.2a on GBM Cell Lines and GBM Cancer Stem Cells. To study the impact

Scheme 5. Synthetic Routes of Amino and Acetamido-D-glycero-D-galactopyranose Analogues

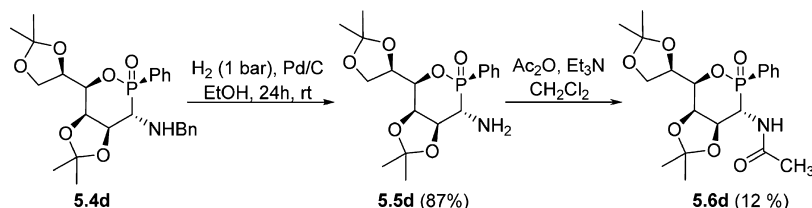


Table 2. Antiproliferative Values (EC_{50} , μM) of the Phostines on CaCo2 (Cell Line Obtained from Colon Cancer Tissue), A431, MDAMB231, B16F1 (Cell Lines Obtained from Skin Cancer Tissues), MDAMB435 (Cell Line Obtained from Breast Cancer Tissue), HuH7 (Cell Line Obtained from Intestine Cancer Tissue), DU145 (Cell Line Obtained from Prostate Cancer Tissue), C6, SNB75, Gli4F11, Gli7 (Cell Lines and Primary Cultures Obtained from Brain Cancer Tissues)^a

	IC_{50} , μM								
	3.1a	3.1b	3.1d	3.2a	3.3a	4.1a	4.2a	4.3a	4.4a
A431	1.11 ± 0.00	0.98 ± 0.00	0.77 ± 0.00	>100	0.55 ± 0.00	>100	4.35 ± 0.40	4.85 ± 1.45	4.44 ± 0.19
CaCo2	>100	>100	>100	>100	>100	>100	>100	>100	>100
MDAMB231	9.37 ± 6.97	6.08 ± 0.46	5.60 ± 0.41	>100	>100	>100	1.16 ± 0.00	3.45 ± 0.13	2.66 ± 0.02
MDAMB435	16.56 ± 0.01	11.02 ± 0.05	11.56 ± 0.24	>100	>100	>100	0.66 ± 0.00	1.96 ± 0.02	4.02 ± 0.00
HuH7	>100	>100	>100	>100	>100	>100	>100	24.01 ± 4.67	>100
B16F10	9.95 ± 5.74	10.18 ± 0.19	10.38 ± 0.06	>100	>100	>100	13.48 ± 0.03	2.08 ± 0.01	1.64 ± 0.00
DU145	>100	>100	>100	>100	>100	>100	>100	>100	>100
C6	0.5 ± 0.00	>100	>100	8.66 ± 0.00	8.62 ± 0.00	10.17 ± 0.00	8.51 ± 0.00	1.11 ± 0.00	6.99 ± 0.00
SNB75	14.33 ± 0.01	13.41 ± 0.01	16.12 ± 0.01	4.92 ± 0.00	6.21 ± 0.00	1.37 ± 0.00	9.54 ± 0.00	6.28 ± 0.00	9.42 ± 0.00
Gli4F11	38.41 ± 1.29	8.56 ± 0.001	11.42 ± 0.01	3.80 ± 0.00	6.12 ± 0.00	8.76 ± 0.00	3.22 ± 0.00	6.81 ± 0.00	5.41 ± 0.00
Gli7	3.16 ± 0.00	3.72 ± 0.00	5.81 ± 0.00	2.50 ± 0.03	2.88 ± 0.00	3.62 ± 0.00	1.93 ± 0.00	2.71 ± 0.00	2.80 ± 0.00
	IC_{50} , μM								
	4.5a	4.6a	4.7a	5.1d	5.2d	5.3d	5.4d	5.5d	5.6d
A431	2.02 ± 0.00	0.84 ± 0.00	>100	1.26 ± 0.00	4.67 ± 1.51	1.34 ± 0.00	4.70 ± 1.37	>100	0.13 ± 0.00
CaCo2	>100	>100	>100	>100	>100	>100	>100	>100	35.96 ± 0.02
MDAMB231	>100	6.35 ± 0.84	4.82 ± 1.30	3.83 ± 0.02	3.72 ± 0.01	9.81 ± 0.00	4.17 ± 0.01	4.15 ± 0.09	23.17 ± 0.01
MDAMB435	>100	2.66 ± 0.01	3.36 ± 0.07	2.48 ± 0.14	2.65 ± 0.02	4.69 ± 0.04	3.99 ± 0.02	1.16 ± 0.01	9.61 ± 0.03
HuH7	>100	23.82 ± 0.00	23.56 ± 0.00	24.21 ± 4.86	23.64 ± 0.00	6.87 ± 0.01	23.80 ± 0.00	16.31 ± 0.00	21.95 ± 0.00
B16F10	>100	2.59 ± 0.17	4.69 ± 1.60	1.96 ± 0.06	2.02 ± 0.01	>100	2.05 ± 0.00	1.02 ± 0.01	14.87 ± 0.01
DU145	>100	>100	>100	>100	>100	>100	>100	>100	31.16 ± 0.01
C6	31.43 ± 4.53	9.44 ± 0.00	9.35 ± 0.01	10.29 ± 0.00	5.50 ± 0.00	5.74 ± 0.00	14.80 ± 0.02	24.42 ± 0.04	0.65 ± 0.00
SNB75	3.11 ± 0.00	6.99 ± 0.02	6.23 ± 0.00	9.99 ± 0.04	5.37 ± 0.00	3.41 ± 0.00	5.16 ± 0.02	2.96 ± 0.02	0.65 ± 0.00
Gli4F11	3.91 ± 0.00	2.87 ± 0.00	2.98 ± 0.00	2.68 ± 0.04	5.55 ± 0.00	5.22 ± 0.20	2.79 ± 0.01	1.37 ± 0.00	0.54 ± 0.00
Gli7	2.07 ± 0.00	1.93 ± 0.00	1.77 ± 0.00	1.82 ± 0.00	2.80 ± 0.00	2.33 ± 0.00	4.62 ± 0.01	1.29 ± 0.01	0.50 ± 0.00

^aValues are calculated from at least three independent experiments. For each set of experiments, each point was repeated six times. IC_{50} estimation was determined with Serf's Cells&Maps software using the Hill equation.

Table 3. Antimigratory Values (K_i) of 3.2a and 5.3d on Gli4, Gli7 Primary Cultures, C6 and SNB75 Cell Lines in a 2D-Migration Assay^a

cell line	K_i , ^b (nM)					
	matrix context, FN		matrix context, VN		matrix context, LN	
	5.3d	3.2a	5.3d	3.2a	5.3d	3.2a
Gli4	31 ± 1	100 ± 1	36 ± 1	194 ± 1	22 ± 1	239 ± 1
GLI7	16 ± 1	64 ± 1	42 ± 1	438 ± 1	100 ± 1	1048 ± 1
SNB75	124 ± 1	19 ± 1	100 ± 1	66 ± 1	60 ± 1	27 ± 1
C6	126 ± 1	27 ± 1	300 ± 1	47 ± 1	77 ± 1	25 ± 1

^aValues are calculated from at least three independent experiments. For each set of experiments, each point was repeated four times. ^b K_i estimation was determined with Serf's Cells&Maps software using the Hill equation.

of 3.2a and 5.3d on GBM cell lines and stem cell cultures migration in the context of the different matrices, we performed all pairwise comparisons of compound–matrix and measured the serum motility response using a 2D-migration assay over the course of 24 h in presence and in absence of the glycomimetics (Table 3). Both 3.2a and 5.3d inhibited the migration of GBM

cancer stem cells and cell lines on matrix made of fibronectin, vitronectin, or laminin. Except for Gli7, inhibition of migration on laminin by 3.2a was in the micromolar range, and the K_i values for migration inhibition were 20–300 times lower than the corresponding EC_{50} for the antiproliferative activity (Tables 2 and 3). Inhibition of migration on fibronectin of Gli4 and Gli7 by

5.3d yielded K_i values of 18 and 13 nM, while EC_{50} antiproliferative values were 5.22 and 2.43 μ M, respectively. Remarkably, **5.3d** had a greater antimigratory activity than **3.2a** against GBM stem cells, whereas **3.2a** had a greater antimigratory effect against GBM cell lines.

Since Gli4 and Gli7 cell lines express stem cell markers such as CD133⁺, CD15⁺, nestin, Sox2, Olig2 and retain the ability to generate neurospheres in vitro,¹⁸ they are considered to represent, like other GBM stem cells, highly relevant cellular models to study human brain tumor initiating cells.¹⁹ Therefore, in the following steps, we focused our attention on the D-glycero-D-galacto-heptopyranose **5.3d** which was more active than **3.2a** on Gli4 and Gli7 migrations.

2.4. The Glycomimetic 5.3d Also Inhibits Cell Invasion.

It is known that qualitative and quantitative differences are observed in cell movements on a planar substratum (2D) and inside an extracellular matrix environment (3D) in response to stimuli by exogenous compounds.²⁰ Therefore, we evaluated the inhibitory effect of **5.3d** on Gli4 and Gli7 migration through a mouse matrigel (Figure 3). The K_i values of 290 and 46 nM for

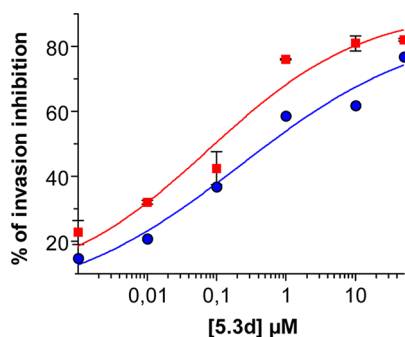


Figure 3. Comparison of **5.3d** invasion inhibition activities on GBM cancer stem cells Gli4 (blue) and Gli7 (red). Curves represent the % of invasion on Gli4 and Gli7 as a function of **5.3d** concentration. Curves were generated using the Serf software.

Gli4 and Gli7 migration inhibitions, respectively, revealed a similar inhibition potential of **5.3d** through a 3D matrix as for a planar substrate. Thus, in a next step in order to validate an in vitro proof of concept, we analyzed the cytotoxic effect of **5.3d** on primary cultures of astrocytes and neurons.

2.5. The Glycomimetic 5.3d Toxicity against Primary Culture of Neurons and Nonproliferative Astrocytes Is Only Observed from 100 μ M. As previously published,¹³ 21-day primary cell cultures of astrocytes were not proliferative, expressed markers of differentiated cells like GFAP, and were not sensitive to AraC. In these experimental conditions, a MTT test revealed that cell cytotoxicity was induced when **5.3d** was used at 100 μ M concentration (Figure 4A). In the same way, on rat neuron primary cultures, propidium iodide (PI) was incorporated only when **5.3d** was used at 100 μ M (Figure 4B,C). At this concentration, the Hoechst nuclei staining was not reduced while the MAP2 immunofluorescence was strongly reduced (Figure 4C). Taken together, these results suggested the initiation of a degenerative process.

With a toxicity starting at 100 μ M on neuron and astrocytes (Figure 4), an antiproliferative activity close to 1 μ M, and antimigratory and invasion activities from 1 nM (Figure 3A,B), **5.3d** has to be considered as a compound with a good in vitro “therapeutic index”.

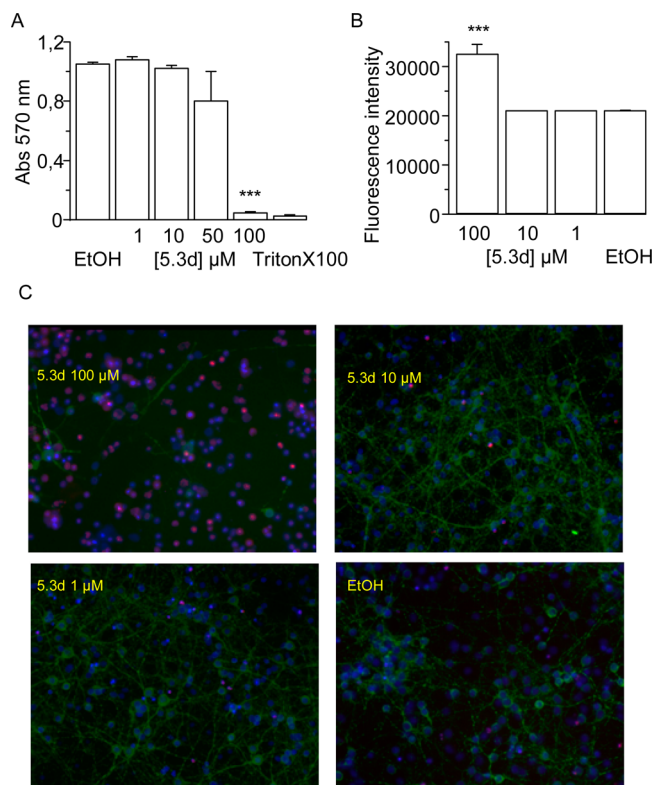


Figure 4. **5.3d** toxicity on nonproliferative astrocytes (A) and neurons (B, C). (A, B) Astrocytes (A) were maintained in cell culture during 2 weeks after isolation from mouse pups cortical brain, and neurons (B) were maintained in culture 3 weeks after isolation from rat embryonic brains (E17) before drug addition. Drug was added for 48 h. (A) Graphics with mean \pm standard deviation from neutral red incorporation measurement. (B) Graphics with mean \pm standard deviation of propidium iodide fluorescence intensities measured at 645 nm with a cytofluor reader from Applied Biosystems. The mean fluorescence was then calculated from three different wells per condition (***) $P < 0,001$. (C) Immunofluorescence study indicating the initiation of a degenerative process at 100 μ M **5.3d**. Map2 (green) was detected using the mouse monoclonal anti MAP-2 (M 9942) from Sigma and revealed with Alexa Fluor 488 (A21206) from invitrogen. Hoechst is shown in blue and propidium iodide in red.

3. DISCUSSION AND CONCLUSION

This one-step synthesis, starting from aryl or alkyl *H*-phosphinates and commercially available protected α -D-mannofuranose, afforded the synthesis of structurally diverse phostines. The purification of the active compounds was achieved by a direct selective precipitation of phostines from the crude mixture or by column chromatography or recrystallization. This methodology allowed an easy scale-up and offered the opportunities to introduce stereochemical modifications leading to different phostines.

The main objective of our screening process was the identification of new C-glycoside analogues inhibiting glioma cell migration and invasion. To reach this goal, we first performed a preliminary screening for antiproliferative activity and a second evaluation based on migration inhibition. We assumed that antimigratory or anti-invasion activities could be combined with an antiproliferative property. However, the cutoff value for the antiproliferative activity fixed at concentrations lower than 10 μ M was not highly stringent. This procedure allowed the

selection of antimigratory compounds without neglecting or, to the contrary, overemphasizing the antiproliferative action.

From the present study, we can conclude that both *D-glycero-D-talo*-heptopyranose and *D-glycero-D-galacto*-heptopyranose analogues inhibited not only GBM cell lines and GBM stem cells proliferation but also that of other types of cancer cell lines. Indeed, melanoma cell line MDAMB435 responds to **4.2a** with an EC_{50} of $0.66 \mu\text{M}$ and a lower antiproliferative concentration of 10 nM . Epidermoid cancers could also be targeted, since the compound **5.6d** inhibits the A431 cell line proliferation with EC_{50} of $0.1 \mu\text{M}$ and a lower antiproliferative concentration of 1 nM .

In a second screening step, we tested the selected glycomimetics **5.3d** and **3.2a** for their migration inhibition activity against GBM cell lines and stem cell cultures. The extracellular matrix (ECM) proteins were selected according to the prominent role they play in the diffusion of glioma cells. Laminin has been localized mainly to the tumor vasculature and at the brain/tumor confrontation zone.²¹ Glioma cells are also known to secrete several laminins.²² Fibronectin is abundant in the brain ECM, and tumor cells have been reported to secrete fibronectin promoting brain tumor progression.²³ Although the normal adult cortex and white matter are devoid of vitronectin, under certain pathological conditions, vitronectin is re-expressed in the brain parenchyma as well as in the endothelial cell basement membrane.²⁴ In accordance with the diffuse feature of glioma, several studies have shown that vitronectin and its receptors enhance glioma motility and invasiveness.²⁵ The lowest K_i values, measured at 24 h, for migration inhibition were 16 nM for **5.3d** against Gli7 fibronectin migration and 19 nM for **3.2a** against SNB75 fibronectin migration (Table 3). The corresponding EC_{50} values, measured at 72 h, were $2.33 \mu\text{M}$ for **5.3d** on Gli7 and $4.92 \mu\text{M}$ for **3.2a** on SNB75 (Table 2). These data indicate a decoupling between migration and proliferation inhibition. They also suggest that the biochemical process that is targeted by **5.3d** and **3.2a** affects both migration and proliferation but has a more predominant action on migration. These compounds can be perceived as C-glycoside mimetics, and their impact on glycosylation will be studied because glycosylation modifications might account for the observed cellular effect on proliferation and migration.²⁶

Interestingly, if **5.3d** is more efficient than **3.2a** in its inhibitory action against GBM stem cells migration (Gli4 and Gli7), **3.2a** is more efficient on GBM cell lines (SNB75 and C6) (Table 3). Because primary cultures of stem cells are more relevant than cell lines as cell models for glioblastoma, compound **5.3d** was selected for further studies. Nonetheless, this difference could also reflect the different patterns of gene expression between the four identified groups of glioblastoma.²⁷ SNB 75 displays prominent mesenchymal features,²⁸ while Gli4 and Gli7 express proneural characteristics.¹⁸ However, both **5.3d** and **3.2a** (data not shown) inhibit Gli4 and Gli7 invasion capacity with the same efficiency.

Finally, the selected hit compound **5.3d** targets CNS cancer cells without affecting normal astrocytes and cortical neurons survival ($>100 \mu\text{M}$). In contrast, we recently published that in the same culture conditions vincristine used at $0.1 \mu\text{M}$ and paclitaxel at $1 \mu\text{M}$ induced astrocyte cytotoxicity.¹³

In conclusion, this work characterized new analogues of C-glycoside targeting CNS cancer migration and invasion without affecting normal astrocytes and cortical neurons survival. This set of data will allow the characterization by preclinical tests of **5.3d** and other compounds of this family.

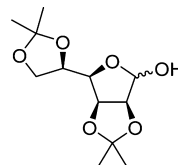
4. EXPERIMENTAL SECTION

4.1. Chemistry. Commercial reagents were purified by distillation or sublimation. The analytical method used to determine the purity of all the compounds described in this paper was the phosphorus, proton NMR, and analytical HPLC. Purity was determined using high performance liquid chromatography (HPLC) carried out on a Shimadzu LC-20AD/T with a Waters column (Waters SunFire C18 $5 \mu\text{m}$, $4.6 \text{ mm} \times 250 \text{ mm}$). The purity of all compounds for biological testing was $\geq 95\%$ in all cases with detection at 254 nm (and 214 nm).

The data for structural refinement of crystallized structures, atomic coordinates, and equivalent isotropic displacement parameters are shown in the Supporting Information.

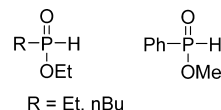
All reactions were carried out under dry nitrogen in flame-dried glassware. Solvents were dried according to current method, distilled, and stored under nitrogen atmosphere. Nuclear magnetic resonance (^1H , ^{31}P , and ^{13}C NMR) spectra were recorded at 400.13 MHz for proton, 161.97 MHz for phosphorus, and 100.6 MHz for carbon (Bruker DRX 400). Low and high resolution mass spectra were acquired using a WATERS Micromass Q-ToF spectrometer with, as internal reference, H_3PO_4 (0.1% in water/acetonitrile, 1/1) in positive mode (ESI). Flash chromatography was performed using a CombiFlash Companion/TS with prepacked column ($6\text{--}120 \text{ g}$ scale) with particle size of $35\text{--}70 \mu\text{m}$.

2.3:5.6-Di-O-isopropylidene- α -D-mannofuranose (**2**).



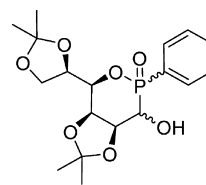
2.3:5.6-Di-O-isopropylidene- α -D-mannofuranose **2** was prepared using the method described by Theodorakis in 1999²⁹ or purchased from Carbosynth Limited. To a suspension of *D*-mannose **2** (50.8 g , 0.28 mol) in acetone (2.5 L) was added iodine (14.21 g , 56 mmol), and the mixture was stirred for 2 h at $25 \text{ }^\circ\text{C}$. The reaction mixture was quenched with sodium thiosulfate (10%) and sodium bicarbonate, and the organic residues were extracted with chloroform. The organic layer was dried over MgSO_4 , concentrated, and crystallized from an hexane/acetone mixture (80/20) to produce **2** (62.4 g , 85%). ^1H NMR (400.13 MHz , CDCl_3): $\delta = 1.34$ (s, 3H), 1.39 (s, 3H), 1.47 (s, 3H), 1.48 (s, 3H), 3.45 (d, 1H, d, $J = 2.4 \text{ Hz}$), 4.08 (dd, 2H, d, $J = 5.5, 1.0 \text{ Hz}$), 4.19 (dd, 1H, $J = 7.0, 3.7 \text{ Hz}$), 4.41 (q, 1H, $J = 5.5 \text{ Hz}$), 4.62 (d, 1H, $J = 5.9 \text{ Hz}$), 4.82 (dd, 1H, $J = 5.9, 3.7 \text{ Hz}$), 5.39 (d, 1H, $J = 2.1 \text{ Hz}$).

General Procedure for Methyl Phenylphosphinate or Ethyl Alkylphosphinate (**1**).



Ethyl alkylphosphinate **1** was prepared using the method described by Petnehazy.³⁰ Methyl arylphosphinate **1** was prepared using the method described by our group.³¹

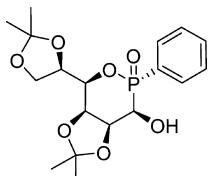
3-Hydroxy-4-(2.2-dimethyl[1.3]dioxolan-4-yl)-2.2-dimethyl-2-oxo-2-phenyltetrahydro-2 λ^5 -[1.2]oxaphosphinanes (**3.1a**–**3.1d**).



2.3:5.6-Di-O-isopropylidene- α -D-mannofuranose **2** (26.25 g , 101.5 mmol) was added under nitrogen to a solution of methyl arylphosphinate **1** (15.84 g , 13.47 mL , 101.5 mmol) in THF (150 mL). Then freshly sublimated potassium *tert*-butoxide (2.28 g , 20.3 mmol) was added to the solution. After a 17 h stirring, the mixture was filtered and the solid was washed with THF. Compound **3.1a** was

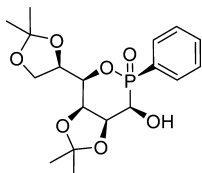
obtained as a white solid (11.8 g, 30%). After filtration, a saturated aqueous solution of sodium chloride was added to the filtrate and the solution was extracted by dichloromethane. After drying of organic layers over sodium sulfate, filtration, and evaporation under vacuum, the final residue was purified by chromatography on silica gel column with as eluent a mixture of ether/ethyl acetate (100/0 to 20/80), affording both different fractions enriched with **3.1b** and **3.1d**. Each fraction was recrystallized in a mixture diethyl ether/pentane, affording compounds **3.1b** (6.81 g, 17%) and **3.1d** (1.8 g, 4%).

(S_pRSRR)-3-Hydroxy-4-(2.2-dimethyl[1.3]dioxolan-4-yl)-2.2-dimethyl-2-oxo-2-phenyltetrahydro-2λ⁵-[1.2]oxaphosphinane (3.1a).



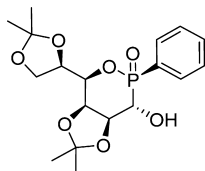
³¹P NMR (161.97 MHz, CDCl₃): δ = 30.43 ppm. ¹H NMR (400.13 MHz, CDCl₃): δ = 1.41 (s, 3H), 1.44 (s, 3H), 1.47 (s, 3H), 1.71 (s, 3H), 3.25 (dd, 1H, *J* = 11.7, 3.1 Hz), 4.04 (dd, 1H, *J* = 11.7, 3.1 Hz), 4.13 (m, 1H), 4.17 (m, 2H), 4.47 (q, 1H, *J* = 12.1, 5.5 Hz), 4.65 (dd, 1H, *J* = 7.9, 1.3 Hz), 4.84 (ddd, 1H, *J* = 24.6, 7.9, 4.1 Hz), 7.50–7.86 (m, 5H) ppm. ¹³C NMR (100.6 MHz, CDCl₃): δ = 24.54, 25.19, 25.60, 26.86, 66.11 (d, *J* = 97.33 Hz), 66.22, 73.27 (d, *J* = 3.7 Hz), 74.44 (d, *J* = 8.0 Hz), 75.25 (d, *J* = 3.7 Hz), 76.20 (d, *J* = 8.0 Hz), 109.78, 111.21, 128.93 (d, *J* = 13.2 Hz), 130.62 (d, *J* = 131.73 Hz), 130.85 (d, *J* = 10.2 Hz), 132.93 ppm. HRMS (ESI) *m/z* calcd for C₁₈H₂₆O₇P (M + H)⁺, 385.1416; found, 385.1404. [α]_D²⁵ +58 (c 10 g/L, MeOH). HPLC: *t*_R = 4.29 min; >99% purity at 254 nm.

(R_pRSRR)-3-Hydroxy-4-(2.2-dimethyl[1.3]dioxolan-4-yl)-2.2-dimethyl-2-oxo-2-phenyltetrahydro-2λ⁵-[1.2]oxaphosphinane (3.1b).



³¹P NMR (161.97 MHz, CDCl₃): δ = 40.00 ppm. ¹H NMR (400.13 MHz, CDCl₃): δ = 1.31 (s, 3H), 1.33 (s, 3H), 1.40 (s, 3H), 1.45 (s, 3H), 4.04–4.14 (m, 2H), 4.17 (dt, 1H, *J* = 8.1, 1.8 Hz), 4.35–4.43 (m, 1H), 4.50–4.60 (m, 2H), 4.77 (ddd, 1H, *J* = 27.0, 7.6, 1.3 Hz), 7.25–7.35 (m, 2H), 7.35–7.50 (m, 1H), 7.85–7.95 (m, 2H) ppm. ¹³C NMR (100.6 MHz, CDCl₃): δ = 24.23, 25.07, 25.65, 27.08, 66.73, 68.48 (d, *J* = 106.8 Hz), 73.56 (d, *J* = 9.5 Hz), 73.85, 74.51 (d, *J* = 5.9 Hz), 75.84, 110.21 (d, *J* = 17.6 Hz), 126.38 (d, *J* = 136.85 Hz), 128.13 (d, *J* = 13.9 Hz), 132.98, 133.25 (d, *J* = 11.0 Hz) ppm. [α]_D²⁵ +56 (c 10 g/L, MeOH). HRMS (ESI) *m/z* calcd for C₁₈H₂₆O₇P (M + H)⁺, 385.1416; found, 385.1424. HPLC: *t*_R = 4.74 min; >95% purity at 254 nm.

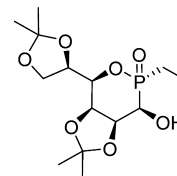
(R_pSSRR)-3-Hydroxy-4-(2.2-dimethyl[1.3]dioxolan-4-yl)-2.2-dimethyl-2-oxo-2-phenyltetrahydro-2λ⁵-[1.2]oxaphosphinane (3.1d).



³¹P NMR (161.97 MHz, CDCl₃): δ = 36.19 ppm. ¹H NMR (400.13 MHz, CDCl₃): δ = 1.40 (s, 3H), 1.42 (s, 3H), 1.47 (s, 3H), 1.49 (s, 3H), 4.14 (d, 1H, *J* = 5.0 Hz), 4.33 (dd, 1H, *J* = 6.6, 3.8 Hz), 4.45 (dt, 1H, *J* = 9.8, 4.2 Hz), 4.54 (ddd, 1H, *J* = 8.1, 6.1, 1.8 Hz), 4.61 (dm, 1H, *J* = 7.3 Hz), 4.88 (ddd, 1H, *J* = 24.5, 7.3, 3.8 Hz), 7.44–7.53 (m, 2H), 7.56–7.65 (m, 1H), 7.88–8.00 (m, 2H) ppm. ¹³C NMR (100.6 MHz, CDCl₃): δ = 24.12, 25.18, 25.76, 26.97, 64.23 (d, *J* = 90.0 Hz), 66.83, 71.90 (d, *J* = 4.4 Hz), 73.59 (d, *J* = 8.1 Hz), 74.00 (d, *J* = 5.1 Hz), 75.36

(d, *J* = 2.9 Hz), 109.71, 110.09, 127.90 (d, *J* = 140.2 Hz), 128.50 (d, *J* = 13.2 Hz), 132.26 (d, *J* = 10.9 Hz), 133.30 (d, *J* = 2.9 Hz) ppm. HRMS (ESI) *m/z* calcd for C₁₈H₂₆O₇P (M + H)⁺, 385.1416; found, 385.1429. [α]_D²⁵ +40 (c 10 g/L, MeOH). HPLC: *t*_R = 5.45 min; >99% purity at 254 nm.

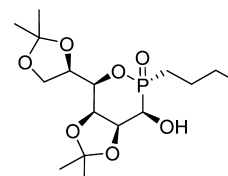
(S_pRSRR)-3-Hydroxy-4-(2.2-dimethyl[1.3]dioxolan-4-yl)-2.2-dimethyl-2-oxo-2-ethyltetrahydro-2λ⁵-[1.2]oxaphosphinane (3.2a).



2.3:5.6-Di-*O*-isopropylidene- α -D-mannofuranose **2** (2 g, 7.68 mmol) was added under nitrogen to a solution of ethyl ethylphosphinate **1** (830 mg, 7.68 mmol) in THF (25 mL), and then freshly sublimated potassium *tert*-butoxide (175 mg, 0.2 equiv) was added to the solution. After a 24 h stirring and addition of a saturated solution of NaCl (25 mL), the mixture was extracted with chloroform (50 mL). **1** was completely consumed and three diastereomers were obtained in 63% yield.

3.2a was separated and recovered pure by chromatography on silica gel with as eluent a mixture of dichloromethane/ethyl acetate (80/20 to 50/50). ³¹P NMR (161.97 MHz, CDCl₃): δ = 46.6 ppm. ¹H NMR (400.13 MHz, CDCl₃): δ = 1.24 (dt, 3H, *J* = 15.2, 7.6 Hz), 1.36 (s, 3H), 1.38 (s, 3H), 1.42 (s, 3H), 1.59 (s, 3H), 1.79–1.97 (m, 2H), 3.69 (dd, 1H, *J* = 10.6, 5.1 Hz), 3.77 (ddd, 1H, *J* = 7.3, 3.1, 1.3 Hz), 3.91 (ddd, 1H, *J* = 10.8, 3.5, 1.8 Hz), 3.99 (dd, 1H, *J* = 9.1, 4.3 Hz), 4.12 (dd, 1H, *J* = 9.1, 6.1 Hz), 4.37 (m, 1H), 4.54 (d, 1H, *J* = 8.8 Hz), 4.79 (ddd, 1H, *J* = 22.7, 7.6, 3.5 Hz) ppm. ¹³C NMR (100.6 MHz, CDCl₃): δ = 5.25 (d, *J* = 5.8 Hz), 20.74 (d, *J* = 90.7 Hz), 24.66, 25.09, 25.72, 26.90, 64.46 (d, *J* = 90.8 Hz), 66.31, 73.32 (d, *J* = 2.9 Hz), 73.96 (d, *J* = 8.8 Hz), 75.37 (d, *J* = 7.3 Hz), 75.65 (d, *J* = 5.1 Hz), 109.79, 110.98 ppm. *m/z* for C₁₄H₂₆O₇P (M + H)⁺: 337.18. HPLC was not possible, as no chromophore group is present for UV detection. Purity was determined using ³¹P NMR, ¹H NMR, and ¹³C NMR.

(S_pRSRR)-3-Hydroxy-4-(2.2-dimethyl[1.3]dioxolan-4-yl)-2.2-dimethyl-2-oxo-2-butyltetrahydro-2λ⁵-[1.2]oxaphosphinane (3.3a).

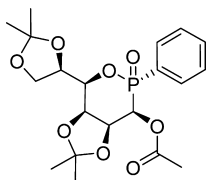


2.3:5.6-Di-*O*-isopropylidene- α -D-mannofuranose **2** (3 g, 11.52 mmol) was added under nitrogen to a solution of ethyl *n*-butylphosphinate **1** (1.56 g, 11.52 mmol) in THF (25 mL), and then freshly sublimated potassium *tert*-butoxide (260 mg, 0.2 equiv) was added to the solution. After 24 h stirring and addition of a saturated solution of NaCl (25 mL), the mixture was extracted with chloroform (50 mL). Compound **1** was completely consumed, and three diastereomers were obtained in 47% yield.

3.3a was separated and recovered pure using normal phase chromatography on silica gel with as eluent a mixture of dichloromethane/ethyl acetate (50/50 to 0/100). ³¹P NMR (161.97 MHz, CDCl₃): δ = 45.43 ppm. ¹H NMR (400.13 MHz, CDCl₃): δ = 0.93 (t, 3H, *J* = 7.3 Hz), 1.36 (s, 3H), 1.38 (s, 3H), 1.42 (s, 3H), 1.43 (sext, 2H, *J* = 7.3 Hz), 1.59 (s, 3H), 1.60–1.97 (m, 4H), 3.35 (dd, 1H, *J* = 10.8, 3.3 Hz), 3.77 (ddd, 1H, *J* = 7.3, 3.0, 1.3 Hz), 3.82 (dd, 1H, *J* = 8.3, 3.3 Hz), 3.98 (dd, 1H, *J* = 9.1, 5.5 Hz), 4.12 (dd, 1H, *J* = 9.1, 6.1 Hz), 4.35 (m, 1H), 4.54 (d, 1H, *J* = 7.8 Hz), 4.76 (ddd, 1H, *J* = 22.9, 7.8, 3.8 Hz) ppm. ¹³C NMR (100.6 MHz, CDCl₃): δ = 13.58, 23.14 (d, *J* = 5.1 Hz), 23.88 (d, *J* = 5.4 Hz), 27.91 (d, *J* = 88.5 Hz), 24.79, 25.08, 25.71, 26.90, 64.95 (d, *J* = 89.3 Hz), 66.37, 73.25 (d, *J* = 2.9 Hz), 73.98 (d, *J* = 8.8 Hz), 75.23 (d, *J* = 7.3 Hz), 75.49 (d, *J* = 4.4 Hz), 109.79, 111.03 ppm. *m/z* for C₁₆H₃₀O₇P (M + H)⁺: 365.19. HPLC was not possible, as no

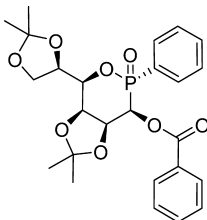
chromophore group is present for UV detection. Purity was determined using ^{31}P NMR, ^1H NMR, and ^{13}C NMR.

(*S_pRSRR*)-3-Acetoxy-4-(2,2-dimethyl[1,3]dioxolan-4-yl)-2,2-dimethyl-2-oxo-2-phenyltetrahydro-2 λ^5 -[1,2]oxaphosphinane (4.1a).



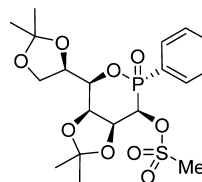
Under dry nitrogen, acetic anhydride (55.3 μL , 0.58 mmol), pyridine (25 μL , 0.39 mmol) and DMAP (4.8 mg, 0.039 mmol) were added to a solution of **3.1a** (150 mg, 0.39 mmol) in dry CH_2Cl_2 (3 mL). The reaction mixture was stirred at room temperature overnight. The organic solution was washed with water and with a saturated aqueous solution of sodium chloride. The combined organic layers were dried over sodium sulfate, filtered, and concentrated under vacuum. The residue was dissolved in a minimum of CH_2Cl_2 and reprecipitated in hexane. **4.1a** was obtained as a white solid with 93% of purity (94 mg, 57%). ^{31}P NMR (161.97 MHz, CDCl_3): δ = 24.7 ppm. ^1H NMR (400.13 MHz, CDCl_3): δ = 1.32 (s, 3H), 1.34 (s, 3H), 1.38 (s, 3H), 1.66 (s, 3H), 2.08 (s, 3H), 4.04 (m, 2H), 4.14 (d, 1H, J = 7 Hz), 4.40 (dd, 1H, J = 12.6 Hz), 4.62 (d, 1H, J = 8 Hz), 4.80 (ddd, 1H, J = 23, 8, 4 Hz), 5.26 (d, 1H, J = 3 Hz), 7.43–7.67 (m, 5H) ppm. ^{13}C NMR (100.61 MHz, CDCl_3): δ = 20.64, 24.37, 25.13, 25.62, 26.88, 66.17, 66.64 (d, J = 54 Hz), 73.49 (d, J = 8.05 Hz), 73.52 (d, J = 9.5 Hz), 74.23 (d, J = 8.0 Hz), 76.95 (d, J = 8.0 Hz), 109.89, 111.51, 129.12 (d, J = 13.9 Hz), 129.93 (d, J = 138.3 Hz), 130.87 (d, J = 10.2 Hz), 133.26 (d, J = 2.2 Hz), 170.23 ppm. HRMS (ESI) m/z calcd for $\text{C}_{20}\text{H}_{28}\text{O}_8\text{P}$ ($M + \text{H}$) $^+$, 427.1528; found, 427.1522. HPLC: t_{R} = 5.89 min; >99% purity at 254 nm.

(*S_pRSRR*)-3-Benzoate-4-(2,2-dimethyl[1,3]dioxolan-4-yl)-2,2-dimethyl-2-oxo-2-phenyltetrahydro-2 λ^5 -[1,2]oxaphosphinane (4.2a).



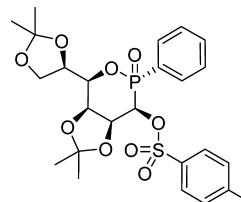
Under dry nitrogen, benzoic anhydride (132 mg, 0.58 mmol), pyridine (25 μL , 0.39 mmol), and DMAP (4.8 mg, 0.039 mmol) were added to a solution of **3.1a** (150 mg, 0.39 mmol) in dry CH_2Cl_2 (3 mL). The reaction mixture was stirred at room temperature overnight. The organic solution was washed with water and with a saturated aqueous solution of sodium chloride. The combined organic layers were dried over sodium sulfate, filtered, and concentrated under vacuum. The residue was dissolved in a minimum of CH_2Cl_2 and reprecipitated in hexane. **4.2a** was obtained as a white solid (149 mg, 78%). ^{31}P NMR (161.97 MHz, DMSO-d_6): δ = 25.02 ppm. ^1H NMR (400.13 MHz, DMSO-d_6): δ = 1.30 (s, 3H), 1.33 (s, 3H), 1.38 (s, 3H), 1.56 (s, 3H), 3.86 (dd, 1H, J = 5.8 Hz), 4.06 (dd, 1H, J = 7.8 Hz), 4.31 (dd, 1H, J = 12.6 Hz), 4.70 (d, 1H, J = 8 Hz), 4.86 (d, 1H, J = 6 Hz), 4.98 (ddd, 1H, J = 24, 8, 4 Hz), 6.00 (d, 1H, J = 4 Hz), 7.53–7.97 (m, 10H) ppm. ^{13}C NMR (100.61 MHz, DMSO-d_6): δ = 24.39, 25.16, 25.62, 26.28, 65.48, 67.16 (d, J = 105.3 Hz), 73.41 (d, J = 8.05 Hz), 73.46 (d, J = 6 Hz), 73.93 (d, J = 8.05 Hz), 75.72 (d, J = 8.05 Hz), 108.79, 109.92, 128.29, 128.68 (d, J = 13.2 Hz), 129.18 (d, J = 51.2 Hz), 130.78 (d, J = 10.2 Hz), 131.28 (d, J = 134.7 Hz), 132.73 (d, J = 2.4 Hz), 134.04, 164.78 ppm. HRMS (ESI) m/z calcd for $\text{C}_{25}\text{H}_{30}\text{O}_8\text{P}$ ($M + \text{H}$) $^+$, 489.1678; found, 489.1669. HPLC: t_{R} = 13.67 min; >99% purity at 254 nm.

(*S_pRSRR*)-3-Acetoxy-4-(2,2-dimethyl[1,3]dioxolan-4-yl)-2,2-dimethyl-2-oxo-2-phenyltetrahydro-2 λ^5 -[1,2]oxaphosphinane (4.3a).

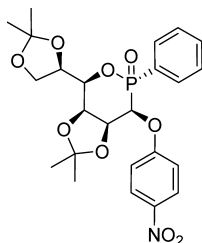


Under dry nitrogen, **3.1a** (1.0 g, 2.4 mmol) was added in distilled pyridine (3 mL, 28 mmol). The reaction mixture was stirred at 0 $^\circ\text{C}$, and then freshly distilled mesyl chloride (2 mL, 24 mmol) was added. After 1 h at 0 $^\circ\text{C}$, the reaction mixture was stirred at room temperature overnight. After addition of chloroform (20 mL), the organic solution was washed with a saturated aqueous solution of sodium bicarbonate (3 \times 10 mL). The combined organic layers were dried over magnesium sulfate, filtered, and concentrated under vacuum. **4.3a** was obtained as a white solid (1.13 g, 99%). ^{31}P NMR (161.97 MHz, CDCl_3): δ = 27.6 ppm. ^1H NMR (400.13 MHz, CDCl_3): δ = 1.29 (s, 3H), 1.35 (s, 3H), 1.38 (s, 3H), 1.53 (s, 3H), 2.91 (s, 3H), 3.85 (dd, 1H, J = 8.8, 4.5 Hz), 3.90 (t, 1H, J = 6.4 Hz), 4.27 (dd, 1H, J = 11.6, 6.3 Hz), 4.68 (dd, 2H, J = 36.1, 8.1 Hz), 5.05 (ddd, 1H, J = 22.9, 8.2, 3.6 Hz), 5.67 (d, 1H, J = 8.0 Hz), 7.59–7.68 (m, 5H) ppm. ^{13}C NMR (100.61 MHz, CDCl_3): δ = 24.30, 25.11, 25.36, 26.15, 37.36, 65.66, 72.57 (d, J = 102.6 Hz), 73.41 (d, J = 5.1 Hz), 73.54 (d, J = 5.1 Hz), 73.72 (d, J = 8.0 Hz), 75.90 (d, J = 8.7 Hz), 108.98, 110.14, 128.76 (d, J = 13.1 Hz), 130.93 (d, J = 109.5 Hz), 131.52 (d, J = 10.0 Hz), 133.23 ppm. HRMS (ESI) m/z calcd for $\text{C}_{19}\text{H}_{28}\text{O}_9\text{PS}$ ($M + \text{H}$) $^+$, 463.1192; found, 463.1175. Mesylate group revealed to be unstable on HPLC and water.

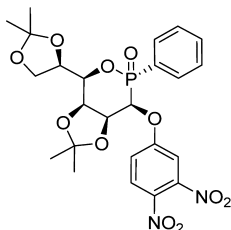
(*S_pRSRR*)-4-(2,2-Dimethyl[1,3]dioxolan-4-yl)-2,2-dimethyl-2-oxo-2-phenyl-3-tosyltetrahydro-2 λ^5 -[1,2]oxaphosphinane (4.4a).



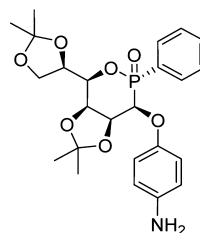
Under dry nitrogen, **3.1a** (1.5 g, 3.6 mmol) was added in distilled pyridine (5 mL, 43 mmol). The reaction mixture was stirred at 0 $^\circ\text{C}$, and then freshly crystallized tosyl chloride (5 g, 36 mmol) was added. After 1 h at 0 $^\circ\text{C}$, the reaction mixture was stirred at room temperature overnight. After addition of chloroform (20 mL), the organic solution was washed with a saturated aqueous solution of sodium bicarbonate (3 \times 10 mL). The combined organic layers were dried over magnesium sulfate, filtered, and concentrated under vacuum. **4.4a** was obtained as a white solid (1.95 g, 95%). ^{31}P NMR (161.97 MHz, CDCl_3): δ = 22.4 ppm. ^1H NMR (400.13 MHz, CDCl_3): δ = 1.29 (s, 3H), 1.37 (s, 3H), 1.44 (s, 3H), 1.69 (s, 3H), 2.38 (s, 3H), 4.02 (m, 2H), 4.24 (d, 1H, J = 7.1 Hz), 4.43 (dd, 1H, J = 8.6, 4.2 Hz), 4.71 (d, 1H, J = 9.1 Hz), 4.83 (d, 1H, J = 8.3 Hz), 5.01 (ddd, 1H, J = 22.9, 3.6 Hz), 7.00–7.58 (m, 9H) ppm. ^{13}C NMR (100.61 MHz, CDCl_3): δ = 21.66, 24.29, 25.12, 25.45, 26.87, 66.15, 72.66 (d, J = 103.2 Hz), 73.56 (d, J = 4.4 Hz), 74.23 (d, J = 6.5 Hz), 74.27, 77.01 (d, J = 8.7 Hz), 109.91, 111.66, 127.78, 128.79, 128.93, 129.43 (d, J = 140.3 Hz), 129.73, 131.27, 131.37, 132.42, 132.98, 145.26. HRMS (ESI) m/z calcd for $\text{C}_{25}\text{H}_{32}\text{O}_9\text{PS}$ ($M + \text{H}$) $^+$, 538.1505; found, 538.1498. Tosylate group was revealed to be unstable on HPLC and water.

(*S_p*,*RS**R**R*)-3-(4-Nitrophenoxy)-4-(2,2-dimethyl[1.3]dioxolan-4-yl)-2,2-dimethyl-2-oxo-2-phenyltetrahydro-2λ⁵-[1.2]-oxaphosphinane (4.5a).**

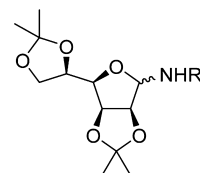
Under dry nitrogen, sodium hydride (50% in oil, 0.08 g, 1.67 mmol) was added to a solution of **3.1a** (0.50 g, 1.3 mmol) in dry THF (10 mL). The reaction mixture was stirred at room temperature for 30 min, and then 4-fluoronitrobenzene (0.183 g, 1.3 mmol) was added. The reaction mixture was stirred for one night. After solvent evaporation under vacuum, chloroform (50 mL) was poured into the crude oil. The organic solution was washed with a saturated aqueous solution of sodium chloride, dried over magnesium sulfate, filtered, and concentrated under vacuum. The residue was purified by chromatography on silica gel using a mixture of CH₂Cl₂/ethyl acetate (100/0 to 0/100) as eluent to give **4.5a** as a white solid (0.591 g, 90%). ³¹P NMR (161.97 MHz, DMSO-*d*₆): δ = 23.9 ppm. ¹H NMR (400.13 MHz, DMSO-*d*₆): δ = 1.43 (s, 6H), 1.49 (s, 3H), 1.77 (s, 3H), 1.60 (s, 3H), 4.21 (d, 2H, *J* = 5.2 Hz), 4.33 (ld, 1H, *J* = 9.3 Hz), 4.54 (q, 1H, *J* = 11.7, 5.5 Hz), 4.78 (m, 2H), 5.01 (ddd, 1H, *J* = 22.4, 7.8, 3.3 Hz), 6.97 (m, 2H), 7.43–7.62 (m, 3H), 7.73–7.81 (m, 2H), 8.09 (m, 2H) ppm. ¹³C NMR (100.61 MHz, DMSO-*d*₆): δ = 24.23, 25.01, 25.47, 26.43, 65.74, 71.49 (d, *J* = 106.2 Hz), 71.81 (d, *J* = 5.8 Hz), 73.38 (d, *J* = 3.7 Hz), 73.79 (d, *J* = 8.0 Hz), 75.86 (d, *J* = 8.1 Hz), 108.92, 110.00, 115.92, 125.79, 128.86 (d, *J* = 13.1 Hz), 130.65 (d, *J* = 10.2 Hz), 131.47 (d, *J* = 133.8 Hz), 141.69, 161.05 (d, *J* = 10.2 Hz) ppm. HRMS (ESI) *m/z* calcd for C₂₄H₂₉NO₉P (M + H)⁺, 506.1580; found, 506.1591. HPLC: *t_R* = 11.73 min; >98% purity at 254 nm.

(*S_p*,*RS**R**R*)-3-(3,4-Dinitrophenoxy)-4-(2,2-dimethyl[1.3]dioxolan-4-yl)-2,2-dimethyl-2-oxo-2-phenyltetrahydro-2λ⁵-[1.2]oxaphosphinane (4.6a).**

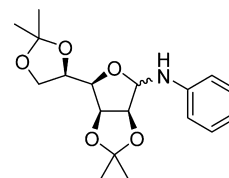
Under dry nitrogen, sodium hydride (50% in oil, 0.08 g, 1.67 mmol) was added to a solution of **3.1a** (0.50 g, 1.3 mmol) in dry THF (10 mL). The reaction mixture was stirred at room temperature for 30 min, and then 3,4-dinitrobenzene (0.321 g, 1.3 mmol) was added. The reaction mixture was stirred for one night. After solvent evaporation under vacuum, chloroform (50 mL) was poured into the crude oil. The organic solution was washed with a saturated aqueous solution of sodium chloride, dried over magnesium sulfate, filtered, and concentrated under vacuum. The residue was purified by chromatography on silica gel using a mixture of CH₂Cl₂/ethyl acetate (100/0 to 0/100) as eluent to give **4.6a** as a white solid (0.651 g, 91%). ³¹P NMR (161.97 MHz, CDCl₃): δ = 26.2 ppm. ¹H NMR (400.13 MHz, CDCl₃): δ = 1.25 (s, 3H), 1.35 (s, 3H), 1.45 (s, 3H), 1.61 (s, 3H), 3.99 (m, 2H), 4.33 (d, 1H, *J* = 5.9 Hz), 4.54 (ls, 1H), 4.86 (d, 1H, *J* = 6.8 Hz), 5.28 (dd, 1H, *J* = 23.0, 6.9 Hz), 5.01 (bs, 1H), 7.39–8.43 (m, 8H) ppm. ¹³C NMR (400.13 MHz, CDCl₃): δ = 24.21, 25.01, 25.41, 26.43, 65.67, 71.63 (d, *J* = 5.8 Hz), 73.47 (d, *J* = 4.4 Hz), 73.71 (d, *J* = 105.5 Hz), 73.82 (d, *J* = 8.0 Hz), 76.01 (d, *J* = 8.7 Hz), 108.96, 110.27, 116.06, 121.22, 128.65, 128.86 (d, *J* = 13.0 Hz), 130.80 (d, *J* = 10.8 Hz), 130.97 (d, *J* = 136.1 Hz), 139.59, 140.75, 153.65 ppm. HRMS (ESI) *m/z* calcd for C₂₄H₂₈O₁₁P (M + H)⁺, 551.1431; found, 551.1432. HPLC: *t_R* = 14.33 min; >97% purity at 254 nm.

(*S_p*,*RS**R**R*)-3-(4-Aminophenoxy)-4-(2,2-dimethyl[1.3]dioxolan-4-yl)-2,2-dimethyl-2-oxo-2-phenyltetrahydro-2λ⁵-[1.2]-oxaphosphinane (4.7a).**

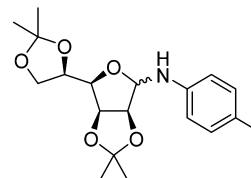
To a 50 mL pressure flask were added sequentially a solution of compound **4.5a** (0.5 g, 1 mmol) in dry ethanol (20 mL) and Pd/C (0.5 g, 0.47 mmol). The system was filled with a hydrogen atmosphere (1 bar). After 24 h stirring at ambient temperature, the reaction mixture was filtered over a Celite pad and the filtrate evaporated under vacuum. The residue was purified by chromatography on silica gel with as eluent a mixture of CH₂Cl₂/ethyl acetate (80/20 to 0/100) as eluent giving **4.7a** (0.455 g, 96%). ³¹P NMR (161.97 MHz, CDCl₃): δ = 39.9 ppm. ¹H NMR (400.13 MHz, CDCl₃): δ = 1.34 (s, 6H), 1.40 (s, 3H), 1.69 (s, 3H), 1.87 (ls, 2H), 4.11 (d, 2H, *J* = 5.3 Hz), 4.24 (ld, 1H, *J* = 7.1 Hz), 4.46 (m, 4H), 4.65 (d, 1H, *J* = 3.3 Hz), 4.68 (ld, 1H, *J* = 7.2 Hz), 4.96 (ddd, 1H, *J* = 22.3, 7.8, 3.2 Hz), 6.87 (m, 2H), 7.38–7.48 (m, 3H), 7.68 (m, 2H), 7.98 (m, 2H) ppm. ¹³C NMR (100.61 MHz, CDCl₃): δ = 25.03, 25.06, 25.28, 26.92, 48.67 (d, *J* = 91.6 Hz), 66.59, 72.77 (d, *J* = 2.9 Hz), 73.29 (d, *J* = 5.1 Hz), 73.96 (d, *J* = 9.4 Hz), 78.21, 109.24, 109.82, 128.59 (d, *J* = 138.2 Hz), 128.82 (d, *J* = 141.8 Hz), 128.50–133.09 (m), 148.04, 153.23 ppm. IR (KBr): 2983, 1642, 1508, 1435, 1373, 1213, 1161, 1120, 1073, 964, 894, 828, 722, 694. HRMS (ESI) *m/z* calcd for C₂₄H₃₁O₇P (M + H)⁺, 476.1838; found, 476.1848. HPLC: *t_R* = 5.39 min; >98% purity at 254 nm.



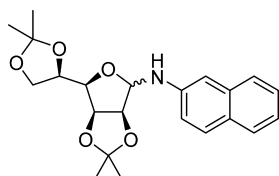
Synthesis was performed according to *Tetrahedron* **1995**, *51*, 4679–4690.

2.3:5.6-Di-O-isopropylidene-1-anilino-α-D-mannofuranose (6.1).

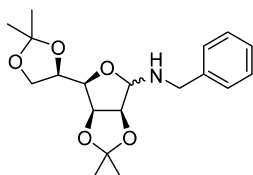
¹H NMR (400.13 MHz, CDCl₃): δ = 1.31 (s, 3H), 1.34 (s, 3H), 1.39 (s, 3H), 1.48 (s, 3H), 3.46 (dd, 1H, *J* = 8.4, 3.3 Hz), 4.02 (m, 2H), 4.37 (qd, 1H, *J* = 8.6, 5.7, 4.5 Hz), 4.63 (dd, 1H, *J* = 6.1, 3.5 Hz), 4.72 (dd, 1H, *J* = 6.1, 3.3 Hz), 4.93 (m, 2H), 6.72–7.13 (m, 5H) ppm.

2.3:5.6-Di-O-isopropylidene-1-(4-toluidino)-α-D-mannofuranose (6.2).

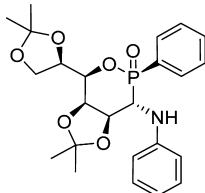
¹H NMR (400.13 MHz, CDCl₃): δ = 1.40 (s, 3H), 1.44 (s, 3H), 1.49 (s, 3H), 1.58 (s, 3H), 2.27 (s, 3H), 3.53 (dd, 1H, *J* = 8.5, 3.3 Hz), 4.12 (m, 2H), 4.47 (m, 1H), 4.71 (q, 1H, *J* = 3.2, 6.0 Hz), 4.82 (q, 1H, *J* = 3.2, 6.0 Hz), 4.91 (d, 1H, *J* = 10.0 Hz), 5.03 (q, 1H, *J* = 3.2, 10.0 Hz), 6.72–7.01 (m, 4H) ppm.

2.3:5.6-Di-O-isopropylidene-1-(2-naphthylamino)- α -D-mannofuranose (6.3).

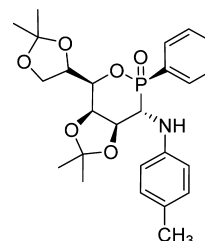
^1H NMR (400.13 MHz, CDCl_3): δ = 1.42 (s, 3H), 1.46 (s, 3H), 1.51 (s, 3H), 1.60 (s, 3H), 3.63 (dd, 1H, J = 16.6, 7.3 Hz), 4.15 (m, 2H), 4.50 (m, 1H), 4.75 (dd, 1H, J = 5.8, 3.6 Hz), 4.82 (dd, 1H, J = 5.8, 3.6 Hz), 5.11 (dd, 1H, J = 13.6, 3.6 Hz), 5.20 (d, 1H, J = 25.2 Hz), 6.90–7.80 (m, 7H) ppm.

2.3:5.6-Di-O-isopropylidene-1-benzylamino- α -D-mannofuranose (6.4).

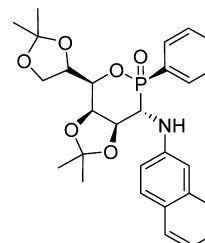
^1H NMR (400.13 MHz, CDCl_3): δ = 1.19 (s, 3H), 1.24 (s, 3H), 1.30 (s, 3H), 1.38 (s, 3H), 3.30 (dd, 1H, J = 7.6, 3.3 Hz), 3.67 (dd, 1H, J = 7.2, 5.9 Hz), 3.81 (dd, 1H, J = 3.8, 2.0 Hz), 3.97 (m, 2H), 4.29 (td, 1H, J = 3.3 Hz), 4.43 (dd, 1H, J = 6.1, 3.5 Hz), 4.53 (dd, 1H, J = 6.1, 3.5 Hz), 4.66 (dd, 1H, J = 5.1, 3.6 Hz), 4.81 (s, 1H), 7.22–7.47 (m, 5H) ppm.

(R_p S $SSRR$)-3-Aminophenyl-4-(2.2-dimethyl[1.3]dioxolan-4-yl)-2.2-dimethyl-2-oxo-2-phenyltetrahydro-2 λ^5 -[1.2]-oxaphosphinane (5.1d).

In a three-neck round-bottom flask under dry nitrogen, mannofuranose **6.1** (1.00 g, 2.98 mmol) was added to a solution of ethyl phenylphosphinate (0.35 mL, 3 mmol) in THF (10 mL), and then freshly sublimated potassium *tert*-butoxide (70 mg, 0.62 mmol, 0.21 equiv) was poured into the solution. The reaction mixture was stirred at room temperature for one night. The crude mixture was washed with a saturated aqueous solution of NaCl. The organic layer was dried over magnesium sulfate, filtered, and concentrated under vacuum. The residue was purified by chromatography on silica gel with as eluent a mixture of *n*-hexane/diethyl ether (100/0 to 0/100) to give **5.1d** (0.80 g, 59%). ^{31}P NMR (161.97 MHz, CDCl_3): δ = 37.1 ppm. ^1H NMR (400.13 MHz, CDCl_3): δ = 1.30 (s, 3H), 1.33 (s, 3H), 1.34 (s, 3H), 1.52 (s, 3H), 3.97 (dd, 1H, J = 7.2, 3.2 Hz), 4.05 (m, 2H), 4.40 (m, 2H), 4.46 (d, 1H, J = 7.1 Hz), 4.77 (qd, 1H, J = 23.0, 7.2, 3.3 Hz), 6.69–6.73 (m, 5H), 7.10–7.37 (m, 5H) ppm. ^{13}C NMR (100.61 MHz, CDCl_3): δ = 24.58, 25.17, 26.25, 27.05, 49.67 (d, J = 85.6 Hz), 66.81, 72.01 (d, J = 3.6 Hz), 73.59 (d, J = 3.6 Hz), 73.66 (d, J = 7.3 Hz), 74.50 (d, J = 2.2 Hz), 109.22, 110.09, 113.59, 119.14, 128.82 (d, J = 141.8 Hz), 128.50, 128.63, 129.46, 132.05, 132.16, 133.35, 146.82. HRMS (ESI) m/z calcd for $\text{C}_{24}\text{H}_{31}\text{NO}_6\text{P}$ ($M + \text{H}$) $^+$, 459.1811; found, 459.1792. HPLC: t_R = 10.46 min; >95% purity at 254 nm.

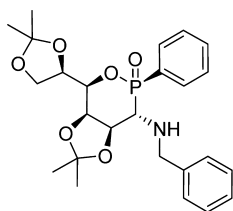
(R_p S $SSRR$)-3-(4-Toluidino)-4-(2.2-dimethyl[1.3]dioxolan-4-yl)-2.2-dimethyl-2-oxo-2-phenyltetrahydro-2 λ^5 -[1.2]-oxaphosphinane (5.2d).

In a three-neck round-bottom flask under dry nitrogen, mannofuranose **6.2** (1 g, 2.86 mmol) was added to a solution of ethyl phenylphosphinate (0.35 mL, 3 mmol) in THF (10 mL), and then freshly sublimated potassium *tert*-butoxide (70 mg, 0.62 mmol) was poured into the solution. The reaction mixture was stirred at room temperature for one night. The crude mixture was washed with a saturated aqueous solution of NaCl. The organic layer was dried over magnesium sulfate, filtered, and concentrated under vacuum. The residue was purified by chromatography on silica gel with as eluent a mixture of *n*-hexane/diethyl ether (100/0 to 0/100) to give **5.2d** (0.71 g, 53%). ^{31}P NMR (161.97 MHz, CDCl_3): δ = 37.9 ppm. ^1H NMR (400.13 MHz, CDCl_3): δ = 1.41 (s, 3H), 1.44 (s, 3H), 1.47 (s, 3H), 1.61 (s, 3H), 2.26 (s, 3H), 4.04 (dd, 1H, J = 10.8, 3.3 Hz), 4.15–4.17 (m, 2H), 4.48–4.49 (m, 2H), 4.56 (d, 1H, J = 16.6 Hz), 4.90 (ddd, 1H, J = 23.0, 7.2, 3.1 Hz), 6.67 (d, 2H, J = 8.4 Hz), 7.03 (d, 2H, J = 8.4 Hz), 7.47–7.70 (m, 3H), 7.98–8.04 (m, 2H) ppm. ^{13}C NMR (100.61 MHz, CDCl_3): δ = 20.39, 24.52, 25.15, 26.18, 27.03, 49.74 (d, J = 86.0 Hz), 66.81, 71.97 (d, J = 3.6 Hz), 73.59 (d, J = 4.2 Hz), 73.64, 109.18, 110.11, 113.68, 128.17, 128.45, 128.59, 129.93, 132.04, 132.15, 144.62, 148.30 ppm. HRMS (ESI) m/z calcd for $\text{C}_{25}\text{H}_{33}\text{NO}_6\text{P}$ ($M + \text{H}$) $^+$, 474.2046; found, 474.2055. HPLC: t_R = 10.26 min; >99% purity at 254 nm.

(R_p S $SSRR$)-3-(2-Aminonaphthyl)-4-(2.2-dimethyl[1.3]dioxolan-4-yl)-2.2-dimethyl-2-oxo-2-phenyltetrahydro-2 λ^5 -[1.2]oxaphosphinane (5.3d).

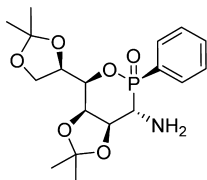
Under dry nitrogen, mannofuranose **6.3** (3.86 g, 10 mmol) was added to a solution of ethyl phenylphosphinate (1.70 mL, 10 mmol) in THF (20 mL), and then freshly sublimated potassium *tert*-butoxide (224 mg, 0.2 mmol, 0.2 equiv) was poured into the solution. The reaction mixture was stirred at room temperature for one night. The crude mixture was washed with a saturated aqueous solution of NaCl. The organic layer was dried over magnesium sulfate, filtered, and concentrated under vacuum. The residue was purified by chromatography on silica gel with as eluent a mixture of CH_2Cl_2 /ethyl acetate (95/5 to 80/20) to give **5.3d** (3.16 g, 62%). ^{31}P NMR (161.97 MHz, CDCl_3): δ = 36.5 ppm. ^1H NMR (400.13 MHz, CDCl_3): δ = 1.35 (s, 3H), 1.38 (s, 3H), 1.39 (s, 3H), 1.57 (s, 3H), 2.26 (s, 3H), 3.71 (dd, 1H, J = 13.6, 10.8 Hz), 4.10–4.10 (m, 2H), 4.42–4.49 (m, 2H), 4.84–5.20 (m, 2H), 6.80–8.00 (m, 12H + 1H) ppm. ^{13}C NMR (100.61 MHz, CDCl_3): δ = 20.59, 25.16, 26.28, 27.06, 49.70 (d, J = 81.1 Hz), 66.84, 72.03 (d, J = 4.4 Hz), 73.59 (d, J = 4.2 Hz), 73.65, 73.70, 74.17, 74.19, 105.04, 109.32, 110.15, 118.70, 122.88, 126.16, 128.82, 129.40 (d, J = 4.4 Hz), 130.18 (d, J = 11.1 Hz), 132.90 (d, J = 14.7 Hz), 134.23 (d, J = 2.9 Hz), 135.55, 145.37 (d, J = 9.6 Hz) ppm. MS m/z $\text{C}_{28}\text{H}_{33}\text{NO}_6\text{P}$ ($M + \text{H}$) $^+$: 510.25. HPLC: t_R = 16.24 min; >95% purity at 254 nm.

(*R*_p*SSRR*)-3-Aminobenzyl-4-(2,2-dimethyl[1,3]dioxolan-4-yl)-2,2-dimethyl-2-oxo-2-phenyltetrahydro-2λ⁵-[1,2]-oxaphosphinane (5.4d).



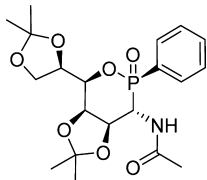
Under dry nitrogen, mannofuranose **6.4** (1 g, 2.86 mmol) was added to a solution of ethyl phenylphosphinate (0.35 mL, 3 mmol) in THF (10 mL), and then freshly sublimated potassium *tert*-butoxide (70 mg, 0.62 mmol) was poured on into the solution. The reaction mixture was stirred at room temperature for one night. The crude mixture was washed with a saturated aqueous solution of NaCl. The organic layer was dried over magnesium sulfate, filtered, and concentrated under vacuum. The residue was purified by chromatography on silica gel with as eluent a mixture of *n*-hexane/diethyl ether (100/0 to 0/100) to give **5.4d** (1 g, 73%). ³¹P NMR (161.97 MHz, CDCl₃): δ = 38.3 ppm. ¹H NMR (400.13 MHz, CDCl₃): δ = 1.35 (s, 3H), 1.37 (s, 3H), 1.40 (s, 3H), 1.45 (s, 3H), 3.35 (dd, 1H, *J* = 7.6, 4.3 Hz), 3.94 (ls, 2H), 4.14 (m, 2H), 4.43 (m, 1H), 4.49 (qd, 1H, *J* = 7.6, 1.8 Hz), 4.58 (m, 1H), 4.69 (ddd, 1H, *J* = 21.2, 6.6, 4.3 Hz), 7.23–7.97 (m, 5H) ppm. ¹³C NMR (100.61 MHz, CDCl₃): δ = 24.66, 25.26, 26.31, 27.01, 52.97 (d, *J* = 87.3 Hz), 53.05, 66.81, 72.56 (d, *J* = 3.6 Hz), 73.70 (d, *J* = 5.1 Hz), 73.81 (d, *J* = 8.7 Hz), 75.47 (d, *J* = 1.5 Hz), 109.10, 110.01, 127.27, 128.14, 128.79, 128.30, 129.57 (d, *J* = 138.9 Hz), 129.60, 131.82, 131.97, 132.87, 138.94 (d, *J* = 17.4 Hz). HRMS (ESI) *m/z* calcd for C₂₅H₃₃NO₆P (M + H)⁺, 474.2046; found, 474.2058. HPLC: *t*_R = 10.22 min; >99% purity at 254 nm.

(*R*_p*SSRR*)-3-Amino-4-(2,2-dimethyl[1,3]dioxolan-4-yl)-2,2-dimethyl-2-oxo-2-phenyltetrahydro-2λ⁵-[1,2]oxaphosphinane (5.5d).



In a 25 mL pressure flask containing the phostine **5.4d** (1 g, 2.11 mmol) in ethanol (10 mL) was added 10 wt % Pd/C (1 g, 0.94 mmol). The system was filled with a hydrogen atmosphere (1 bar). After 24 h stirring at ambient temperature, reaction mixture was filtered over a Celite pad and the filtrate evaporated under vacuum. The residue was purified by chromatography on silica gel with as eluent a mixture of diethyl ether/ethanol (100/0 to 80/20) to give **5.5d** (0.7 g, 87%). ³¹P NMR (161.97 MHz, CDCl₃): δ = 37.46 ppm. ¹H NMR (400.13 MHz, CDCl₃): δ = 1.38 (s, 3H), 1.41 (s, 3H), 1.44 (s, 3H), 1.50 (s, 3H), 1.86 (ls, 2H), 3.49 (dd, 1H, *J* = 6.4, 5.2 Hz), 4.11 (m, 2H), 4.39–4.58 (m, 4H), 7.39–7.87 (m, 5H) ppm. ¹³C NMR (100.61 MHz, CDCl₃): δ = 25.04, 25.27, 26.93, 26.95, 48.78 (d, *J* = 91.6 Hz), 66.78, 72.85 (d, *J* = 3 Hz), 73.27 (d, *J* = 5.1 Hz), 73.97 (d, *J* = 9.5 Hz), 78.33, 109.23, 109.96, 128.71 (d, *J* = 138 Hz), 128.41, 128.52, 131.92, 132.02, 133.02. HRMS (ESI) *m/z* calcd for C₁₈H₂₇NO₆P (M + H)⁺, 384.1576; found, 384.1567. HPLC: *t*_R = 4.86 min; >99% purity at 254 nm.

(*R*_p*SSRR*)-3-Acetamide-4-(2,2-dimethyl[1,3]dioxolan-4-yl)-2,2-dimethyl-2-oxo-2-phenyltetrahydro-2λ⁵-[1,2]-oxaphosphinane (5.6d).



Under dry nitrogen, acetic anhydride (72 μL, 0.76 mmol) and triethylamine (60 μL, 0.42 mmol) were added to a solution of **5.5d** (145 mg, 0.38 mmol) in dry CH₂Cl₂ (5 mL). The reaction mixture was stirred at room temperature for 2 h. The organic solution was washed with a saturated aqueous solution of sodium bicarbonate. The combined organic layers were dried over sodium sulfate, filtered, and concentrated under vacuum. The residue was purified by chromatography on silica gel using a mixture of heptane/ethyl acetate/EtOH (50/50/0 to 0/95/5) as eluent to give a white solid. This product was dissolved in a minimum of Et₂O and reprecipitated in hexane. **7.1d** was obtained as a white solid (20 mg, 12%). ³¹P NMR (161.97 MHz, CDCl₃): δ = 37.02 ppm. ¹H NMR (400.13 MHz, CDCl₃): δ = 1.31 (s, 3H), 1.34 (s, 3H), 1.37 (s, 3H), 1.53 (s, 3H), 1.91 (s, 3H), 4.03 (ddd, 2H, *J* = 4.5, 5.5, 9 Hz), 4.36–4.48 (m, 3H), 4.60–4.71 (m, 2H), 6.74 (sl, 1H), 7.42–7.88 (m, 5H) ppm. ¹³C NMR (100.61 MHz, CDCl₃): δ = 25.59, 26.41, 26.85, 27.51, 66.61, 68.01, 68.97, 74.72, 75.09, 75.17, 76.86, 76.93, 109.88, 111.04, 129.70, 130.03, 130.54, 131.92, 133.87, 135.50, 165.98. HRMS (ESI) *m/z* calcd for C₂₀H₃₀NO₇P (M + H)⁺, 426.1682; found, 426.1686. HPLC: *t*_R = 3.57 min; >96% purity at 254 nm.

4.2. Cell Cultures. Cell Lines. A431, MDAMB231, DU145, MDAMB435, B16F10, CaCo2, and HuH7 cells were obtained from the American Type Culture Collection. The C6 cells were a gift from M. Mersel (INM). These cell lines were cultured in Dulbecco's modified Eagle medium (DMEM, Fisher Scientific, France) supplemented with 10% heat inactivated fetal calf serum (FCS, Fisher Scientific, France), 2 mM L-glutamine (Fisher Scientific, France), 1 mM sodium pyruvate (Sigma France), and 50 U mL⁻¹ streptomycin (Fisher Scientific, France).

Astrocytes. Astrocytes were isolated from newborn mice (day 2) cortex as previously described.³²

Cortical Neurons. Neurons were isolated from rat embryonic cortex (E17) and cultured 17 days as previously described.³³

GBM Primary Cultures. Isolation and culture of GBM cells using the classical nonadherent NS method were performed according to a protocol used to derive NS from the adult human spinal cord as described in Dromard et al.³⁴ and adapted by Guichet et al. for Gli4 and Gli7.¹⁸

Drug Addition. Cytosine arabinoside (AraC), dimethylthiazolyl-2,5-diphenyltetrazolium bromide (MTT), neutral red, phosphate buffer saline (PBS), Triton X-100, Hoechst 33342, and propidium iodide were purchased from Sigma. Phostine solutions were prepared in 100% DMSO. AraC at 10 μM was prepared in PBS.

4.3. Measurements of Phostine Effects on Cancer Cell Line Cultures and GBM, Astrocytes and Neurons Primary Cultures, Proliferation, and Survival. MTT Assay. The MTT assay was carried out as previously described at 48 and 72 h after drug addition.³⁵

Neutral Red Assay. The neutral red assay was carried out as previously described³⁵ 48 h after drug addition.³⁶

Hoechst 33342 and Propidium Iodide Fluorescence Measurements. After 48 h of phostine treatment, 5 μg/mL Hoechst 33342 and 10 μM of propidium iodide were added in the culture medium for 30 min at 37 °C. Cells were then washed in PBS and fixed during 10 min with 4% paraformaldehyde. The mean fluorescence at four positions in each well at 460 nm was measured (Cytofluor multiwell plate reader 4000, PerSeptive Biosystems) with excitation at 360 nm and a gain of 90 dB. The mean fluorescence of three wells per condition was then calculated. Fluorescence was detected with an ORCA camera (ORCA ER;0.63), with a ×20 objective and a XF 93 filter and a gain of 25 dB. Exposure times were 24 and of 280 ms for Hoechst 33342 and propidium iodide, respectively. Control fluorescence intensities for red and blue staining were measured on Triton X-100 (2%) treated cells. The mean percentage of propidium iodide incorporation was calculated from three different wells per condition.

4.4. Measurements of Phostine Effects on GBM Cancer Cell Line Cultures (SNB75, C6) and GBM Primary Cultures (Gli4, Gli7), Migration, and Invasion. For migration, inserts of boyden chambers (no. 353504 BD Biosciences) were coated overnight with 20 μg/mL of either laminin (no. 354232 BD Biosciences), fibronectin (no. 354008 BD Biosciences), or vitronectin (no. 354238 BD Biosciences) (human plasma, BD Biosciences) washed in PBS and blocked with 0.5%

BSA for 1 h. For invasion 100 μ L of Matrigel (BD Matrigel matrix, mouse EHS tumor, LDEV; no. 356234 BD Biosciences) diluted 33 times in PBS was added in the inset. Cells (50×10^5) resuspended in DMEM supplemented with 0.1% BSA were plated into the upper compartment and incubated for 24 h with and without treatment. For Gli4 and Gli7 cells were recovered from neurospheres obtained from nonadhesive culture conditions. Cell culture medium (0.5 mL) containing 10% of FCS was placed in the lower compartment to facilitate chemoattraction. The upper side of the filter was wiped off to remove nonmigrating cells, and cells attached to the lower side were fixed for 10 min with methanol, stained with crystal violet, and fully counted using a Zeiss axiophot microscope ($\times 200$). The percentage of migration inhibition (% Inh) was calculated as follows: % Inh = $100 - (\text{number of cell migrating without treatment} / \text{number of cell migrating under treatment}) \times 100$.

4.5. Statistical Analyses. The presented experiments were carried out at least in triplicate, depending on the number of independent variables. Student's or ANOVA statistical tests were applied, using Serf software (bram.org/serf/CellsAndMaps.php). EC_{50} values and K_i were calculated using the Hill equation of the dose–log response curves.

■ ASSOCIATED CONTENT

📄 Supporting Information

Experimental procedures for compound synthesis and characterization data. This material is available free of charge via the Internet at <http://pubs.acs.org>.

■ AUTHOR INFORMATION

Corresponding Authors

*J.-L.P.: e-mail, jean-luc.pirat@enscm.fr; phone, +33 467 147 243; fax, +33 467 144 313.

*N.B.: e-mail, norbert.bakalara@enscm.fr; phone, +33 607 106 844; fax, +33 499 636 020.

Author Contributions

¹L.C. and C.J. equally contributed to the paper.

Notes

The authors declare no competing financial interest.

■ ACKNOWLEDGMENTS

We thank Adina Hamdouchi, Damien Filippini, Marysa Teiggle for expert technical support, and Patrick Carroll, Leonidas Iasemidis, and Zsofia Sforza for carefully reading the manuscript and for English language. This research was supported by MRT, ANR (INSERM), and L'Ecole Nationale Supérieure de Chimie de Montpellier (ENSCM).

■ ABBREVIATIONS USED

EC_{50} , half maximal effective concentration; MRI, magnetic resonance imaging; MTT, dimethylthiazolyl-2,5-diphenyltetrazolium bromide; LTC, lower toxic concentration; GP, growth percent; AraC, cytarabine or cytosine arabinoside; GFAP, glial fibrillary acidic protein; PI, propidium iodide; LDH, lactate dehydrogenase; CH_2Cl_2 , dichloromethane; HPLC, high performance liquid chromatography; INM, Institut des Neurosciences de Montpellier; DMEM, Dulbecco's modified Eagle medium; MAP2, microtubule associated protein 2; GBM, glioblastoma multiform; FCS, fetal calf serum; DMSO, dimethylsulfoxide; CNS, central nervous system; LGG, low-grade glioma; FLAIR, fluid attenuated inversion recovery; MRI, magnetic resonance imaging; H-RAS, Harvey rat sarcoma viral oncogene homolog; HGF/MET, hepatocyte growth factor/Met tyrosine kinase; PI3K, phosphoinositide 3-kinase; MAPK, mitogen-activated protein kinase; NCI/NIH, National Cancer

Institute/National Institutes of Health; NMR, nuclear magnetic resonance

■ REFERENCES

- (1) Duffau, H. Surgery of low-grade gliomas: towards a "functional neurooncology". *Curr. Opin. Oncol.* **2009**, *21*, 543–549.
- (2) Soffietti, R.; Baumert, B. G.; Bello, L.; von Deimling, A.; Duffau, H.; Frenay, M.; Grisold, W.; Grant, R.; Graus, F.; Hoang-Xuan, K.; Klein, M.; Melin, B.; Rees, J.; Siegal, T.; Smits, A.; Stupp, R.; Wick, W. Guidelines on management of low-grade gliomas: report of an EFNS-EANO Task Force. *Eur. J. Neurol.* **2009**, *17*, 1124–1133.
- (3) Yordanova, Y. N.; Moritz-Gasser, S.; Duffau, H. Awake surgery for WHO grade II gliomas within "noneloquent" areas in the left dominant hemisphere: toward a "supratotal" resection. *Clinical article. J. Neurosurg.* **2011**, *115*, 232–239.
- (4) De Benedictis, A.; Moritz-Gasser, S.; Duffau, H. Awake mapping optimizes the extent of resection for low-grade gliomas in eloquent areas. *Neurosurgery* **2010**, *66*, 1074–1084.
- (5) Chamberlain, M. C. Radiographic patterns of relapse in glioblastoma. *J. Neuro-Oncol.* **2011**, *101*, 319–323.
- (6) Sampetean, O.; Saga, I.; Nakanishi, M.; Sugihara, E.; Fukaya, R.; Onishi, N.; Osuka, S.; Akahata, M.; Kai, K.; Sugimoto, H.; Hirao, A.; Saya, H. Invasion precedes tumor mass formation in a malignant brain tumor model of genetically modified neural stem cells. *Neoplasia* **2011**, *13*, 784–791.
- (7) McLendon, R. E.; Rich, J. N. Glioblastoma stem cells: a neuropathologist's view. *J. Oncol.* **2011**, No. 397195, DOI: 10.1155/2011/397195.
- (8) Duffau, H.; Taillandier, L.; Capelle, L. Radical surgery after chemotherapy: a new therapeutic strategy to envision in grade II glioma. *J. Neuro-Oncol.* **2006**, *80*, 171–176.
- (9) Kotliarova, S.; Fine, H. A. SnapShot: glioblastoma multiforme. *Cancer Cell* **2012**, *21*, 710–710.
- (10) Dhruv, H. D.; McDonough Winslow, W. S.; Armstrong, B.; Tuncali, S.; Eschbacher, J.; Kislin, K.; Loftus, J. C.; Tran, N. L.; Berens, M. E. Reciprocal activation of transcription factors underlies the dichotomy between proliferation and invasion of glioma cells. *PLoS One* **2013**, *8*, e72134.
- (11) Kim, H. D.; Guo, T. W.; Wu, A. P.; Wells, A.; Gertler, F. B.; Lauffenburger, D. A. Epidermal growth factor-induced enhancement of glioblastoma cell migration in 3D arises from an intrinsic increase in speed but an extrinsic matrix- and proteolysis-dependent increase in persistence. *Mol. Biol. Cell* **2008**, *19*, 4249–4259.
- (12) Cecchi, F.; Rabe, D. C.; Bottaro, D. P. Targeting the HGF/Met signaling pathway in cancer therapy. *Expert Opin. Ther. Targets* **2012**, *16*, 553–572.
- (13) Clarion, L.; Jacquard, C.; Sainte-Catherine, O.; Loiseau, S.; Filippini, D.; Hirtle, M. H.; Volle, J. N.; Virieux, D.; Lecouvey, M.; Pirat, J. L.; Bakalara, N. Oxaphosphinanes: new therapeutic perspectives for glioblastoma. *J. Med. Chem.* **2012**, *55*, 2196–2211.
- (14) Darrow, J. W.; Drueckhammer, D. G. Cyclic phosphonate analogs of hexopyranoses. *J. Org. Chem.* **1994**, *59*, 2976–2985.
- (15) Cristau, H.-J.; Monbrun, J.; Schleiss, J.; Virieux, D.; Pirat, J.-L. First synthesis of P-aryl-phosphinosugars, organophosphorus analogues of C-aryl glycosides. *Tetrahedron Lett.* **2005**, *46*, 3741–3744.
- (16) Cipolla, L.; Lay, L.; Nicotra, F.; C, P.; L, P. Synthesis of azasugars by Grignard reaction on glycosylamines. *Tetrahedron* **1995**, *51*, 4679–4690.
- (17) Behr, J. M.; Guillerme, G. Synthesis of 6-deoxy-homoDMDP and its C(5)-epimer: absolute stereochemistry of natural products from *Hyacinthus orientalis*. *Tetrahedron: Asymmetry* **2002**, *13*, 111–113.
- (18) Guichet, P. O.; Bieche, I.; Teigell, M.; Serguera, C.; Rothhut, B.; Rigau, V.; Scamps, F.; Vacher, S.; Ripoll, C.; Taviaux, S.; Chevassus, H.; Duffau, H.; Mallet, J.; Susini, A.; Joubert, D.; Bauchet, L.; Hugnot, J. P. Cell death and neuronal differentiation of glioblastoma stem-like cells induced by neurogenic transcription factors. *Glia* **2012**, *61*, 225–239.
- (19) Singh, S. K.; Hawkins, C.; Clarke, I. D.; Squire, J. A.; Bayani, J.; Hide, T.; Henkelman, R. M.; Cusimano, M. D.; Dirks, P. B.

Identification of human brain tumour initiating cells. *Nature* **2004**, *432*, 396–401.

(20) Fraley, S. I.; Feng, Y.; Krishnamurthy, R.; Kim, D.-H.; Celedon, A.; Longmore, G. D.; Wirtz, D. A distinctive role for focal adhesion proteins in threedimensional cell motility. *Nat. Cell Biol.* **2010**, *12*, 598–604.

(21) Mahesparan, R.; Read, T. A.; Lund-Johansen, M.; Skafnesmo, K. O.; Bjerkvig, R.; Engebraaten, O. Expression of extracellular matrix components in a highly infiltrative in vivo glioma model. *Acta Neuropathol.* **2003**, *105*, 49–57.

(22) Kawataki, T.; Yamane, T.; Naganuma, H.; Rousselle, P.; Anduren, I.; Tryggvason, K.; Patarroyo, M. Laminin isoforms and their integrin receptors in glioma cell migration and invasiveness: evidence for a role of alpha5-laminin(s) and alpha3beta1 integrin. *Exp. Cell Res.* **2007**, *313*, 3819–3831.

(23) Sengupta, S.; Nandi, S.; Hindi, E. S.; Wainwright, D. A.; Han, Y.; Lesniak, M. S. Short hairpin RNA-mediated fibronectin knockdown delays tumor growth in a mouse glioma model. *Neoplasia* **2010**, *12*, 837–847.

(24) Uhm, J. H.; Dooley, N. P.; Kyritsis, A. P.; Rao, J. S.; Gladson, C. L. Vitronectin, a glioma-derived extracellular matrix protein, protects tumor cells from apoptotic death. *Clin. Cancer Res.* **1999**, *5*, 1587–1594.

(25) Gladson, C. L.; Wilcox, J. N.; Sanders, L.; Gillespie, G. Y.; Cheresch, D. A. Cerebral microenvironment influences expression of the vitronectin gene in astrocytic tumors. *J. Cell Sci.* **1995**, *108*, 947–956.

(26) Hakomori, S. Glycosylation defining cancer malignancy: new wine in an old bottle. *Proc. Natl. Acad. Sci. U.S.A.* **2002**, *99*, 10231–10233.

(27) Verhaak, R. G.; Hoadley, K. A.; Purdom, E.; Wang, V.; Qi, Y.; Wilkerson, M. D.; Miller, C. R.; Ding, L.; Golub, T.; Mesirov, J. P.; Alexe, G.; Lawrence, M.; O'Kelly, M.; Tamayo, P.; Weir, B. A.; Gabriel, S.; Winckler, W.; Gupta, S.; Jakkula, L.; Feiler, H. S.; Hodgson, J. G.; James, C. D.; Sarkaria, J. N.; Brennan, C.; Kahn, A.; Spellman, P. T.; Wilson, R. K.; Speed, T. P.; Gray, J. W.; Meyerson, M.; Getz, G.; Perou, C. M.; Hayes, D. N. Integrated genomic analysis identifies clinically relevant subtypes of glioblastoma characterized by abnormalities in PDGFRA, IDH1, EGFR, and NF1. *Cancer Cell* **2010**, *17*, 98–110.

(28) Ross, D. T.; Scherf, U.; Eisen, M. B.; Perou, C. M.; Rees, C.; Spellman, P.; Iyer, V.; Jeffrey, S. S.; Van de Rijn, M.; Waltham, M.; Pergamenschikov, A.; Lee, J. C.; Lashkari, D.; Shalon, D.; Myers, T. G.; Weinstein, J. N.; Botstein, D.; Brown, P. O. Systematic variation in gene expression patterns in human cancer cell lines. *Nat. Genet.* **2000**, *24*, 227–235.

(29) Kim, C.; Hoang, R.; Theodorakis, E. A. Synthetic studies on norrisolide: enantioselective synthesis of the norrisane side chain. *Org. Lett.* **1999**, *1*, 1295–1297.

(30) Petnehazy, I.; Jaszay, Z. M.; Szabo, A.; Everaert, K. Convenient one-pot synthesis of phosphonites and H-phosphinates. *Synth. Commun.* **2003**, *33*, 1665–1674.

(31) Afarinkia, K.; Yu, H. W. Hewitt reaction revisited. *Tetrahedron Lett.* **2003**, 781–783.

(32) Audouy, S.; Mallet, J.; Privat, A.; Gimenez y Ribotta, M. Adenovirus-mediated suicide gene therapy in an in vitro model of reactive gliosis. *Glia* **1999**, *25*, 293–303.

(33) Drian, M. J.; Kamenka, J. M.; Pirat, J. L.; Privat, A. Non-competitive antagonists of *N*-methyl-D-aspartate prevent spontaneous neuronal death in primary cultures of embryonic rat cortex. *J. Neurosci. Res.* **1991**, *29*, 133–138.

(34) Dromard, C.; Guillon, H.; Rigau, V.; Ripoll, C.; Sabourin, J. C.; Perrin, F. E.; Scamps, F.; Bozza, S.; Sabatier, P.; Lonjon, N.; Duffau, H.; Vachier-Lahaye, F.; Prieto, M.; Tran Van Ba, C.; Deleyrolle, L.; Boularan, A.; Langley, K.; Gaviria, M.; Privat, A.; Hugnot, J. P.; Bauchet, L. Adult human spinal cord harbors neural precursor cells that generate neurons and glial cells in vitro. *J. Neurosci. Res.* **2008**, *86*, 1916–1926.

(35) Mosmann, T. Rapid colorimetric assay for cellular growth and survival: application to proliferation and cytotoxicity assays. *J. Immunol. Methods* **1983**, *65*, 55–63.

(36) Repetto, G.; del Peso, A.; Zurita, J. L. Neutral red uptake assay for the estimation of cell viability/cytotoxicity. *Nat. Protoc.* **2008**, *3*, 1125–1131.